

SYNTHESIS OF NANOMEDICINE FOR COMBATING GLAUCOMA

M.Tech. Thesis

By
MD BELAL HOSSAIN



**DEPARTMENT OF BIOSCIENCES & BIOMEDICAL
ENGINEERING
INDIAN INSTITUTE OF TECHNOLOGY INDORE
MAY 2025**

SYNTHESIS OF NANOMEDICINE FOR COMBATING GLAUCOMA

A THESIS

*Submitted in partial fulfillment of the
requirements for the award of the degree*

of
Master of Technology

by
MD BELAL HOSSAIN



**DEPARTMENT OF BIOSCIENCES & BIOMEDICAL
ENGINEERING
INDIAN INSTITUTE OF TECHNOLOGY INDORE
MAY 2025**

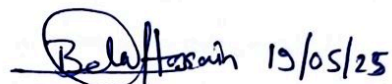


INDIAN INSTITUTE OF TECHNOLOGY INDORE

CANDIDATE'S DECLARATION

I hereby certify that the work which is being presented in the thesis entitled **SYNTHESIS OF NANOMEDICINE FOR COMBATING GLAUCOMA** in the partial fulfillment of the requirements for the award of the degree of **MASTER OF TECHNOLOGY** and submitted in the **DEPARTMENT OF BIOSCIENCES AND BIOMEDICAL ENGINEERING, Indian Institute of Technology Indore**, is an authentic record of my own work carried out during the time period from July 2023 to May 2025 under the supervision of Dr. Abhijeet Joshi, Associate Proffesor, Department of Biosciences & Biomedical Engineering.

The matter presented in this thesis has not been submitted by me for the award of any other degree of this or any other institute.

 19/05/25

Signature of the student with date
MD BELAL HOSSAIN

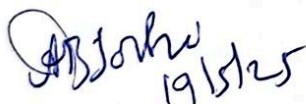
This is to certify that the above statement made by the candidate is correct to the best of my/our knowledge.

 19/5/25

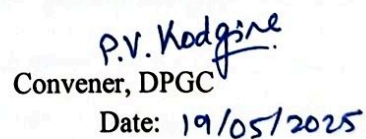
Signature of the Supervisor with date

DR. ABHIJEET JOSHI

MD BELAL HOSSAIN has successfully given his M.Tech. Oral Examination held on **5th May**.

 19/5/25

Signature of Supervisor of M.Tech. thesis
Date:


Convener, DPGC
Date: 19/05/2025

ACKNOWLEDGEMENTS

When I started this journey, I had little to no experience working in a lab environment. Completing this project wouldn't have been possible without the support and encouragement of many people here, and I'm sincerely grateful to everyone who, in one way or another, helped me learn and grow throughout this research experience. I'd especially like to thank my project supervisor, **Dr. Abhijeet Joshi**, for his unwavering patience and guidance. He never hesitated to correct my mistakes—no matter how small—and took the time to teach me the fundamentals that are essential not just in research, but in any professional setting. Our discussions, whether about the project or broader life lessons, were always insightful and encouraging. His calm demeanor and thoughtful approach left a lasting impression on me, and I've gained not only research skills but also valuable life lessons under his mentorship. Working with him has truly been a transformative and memorable experience.

I'm deeply grateful to **Badri Narayana Sahoo** who treated me like a brother and guided me every step of the way. From teaching me essential lab techniques to supporting me through challenges, their mentorship was instrumental in helping me complete this master's research journey. I truly couldn't have imagined reaching this point without them. Their knowledge, dedication, and constant encouragement not only shaped my work but also played a key role in my personal and academic growth. I especially thank him for his patience and for believing in me—even during times when I struggled to believe in myself.

I'm incredibly thankful to **Simran Rana**, who supported me throughout this journey. From patiently teaching me core lab techniques to helping me navigate the inevitable challenges, her guidance was truly invaluable. I honestly can't imagine completing this master's research without her support. Their expertise, commitment, and continuous encouragement not

only helped me grow as a researcher but also had a lasting impact on my personal development.

I would also like to express my heartfelt thanks to my seniors — **Surbhi Jaiswal** for teaching me the operation of HPLC, and **Parul Yadav** for teaching the operation of Rheometer and their constant support and guidance throughout this journey.

I'm also grateful to my fellow lab members—for their unwavering support and guidance throughout this journey.

I would like to sincerely thank the **BSBE department**, especially **Mr. Arif Patel, Mr. Gaurav Singh, and Mr. Amit Kumar**, as well as **SIC, IIT Indore**, for providing the necessary instrumental facilities that made this research possible.

I'm also deeply thankful to my friends — **Surjya Pratap Sarangi, Reetam Sarkar, Jayant Kashyap, Nandini Singh, Pradeep Kumar, and Advait Sohani** — for standing by me through all the highs and lows. Their companionship, encouragement, and good humor made this journey not just bearable, but truly memorable.

I am profoundly grateful to the foundation of my life — my parents, **Mr. Md. Abarak Hossain and Mrs. Mst Waheda Bibi** — for their unwavering love, care, and the values they've instilled in me. Their constant support and belief in my abilities have been the driving force behind everything I've achieved. I also want to sincerely thank my siblings, **Mst Halima Khatun and Md. Usuf Ali**, for always understanding and motivating me. Without their strength and encouragement, I wouldn't be where I am today.

Dedicated to my Parents
Mr. Md. Abarak Hossain
And
Mrs. Mst Waheda Bibi

Abstract

Eye diseases such as glaucoma significantly impact the adult population. Glaucoma primarily impacts older adults, and is characterized by an increase in intra-ocular pressure due to the restricted drainage of aqueous humor, which leads to damage of the optic nerve. Delivering medication to the eye is difficult due to several barriers. In-situ gelling systems, applied topically, are increasingly popular in ocular treatments. These systems offer a promising way to improve how we treat various eye conditions. These challenges include the eye's natural defenses, such as tear production and blinking, which can quickly remove medications. Additionally, the cornea, the eye's outermost layer, is designed to prevent foreign substances from entering, further complicating drug absorption. Overcoming these obstacles is crucial for effective treatment. In-situ gelling systems are liquid formulations that turn into a gel once in contact with the eye. This transition is triggered by changes in pH, or the presence of ions in the tear fluid. The gel-like consistency helps the medication stay on the eye's surface longer, allowing for better absorption and more effective treatment. In this study, we have developed a drug-loaded nanoparticle system incorporated into an ion-activated in situ gel to achieve sustained drug release. The use of the in-situ gel formulation aims to minimize drug loss, which typically occurs due to tear fluid secretion and eye blinking, thereby enhancing the retention time of the drug in the ocular region. Polymeric nanoparticles loaded with the drug are used for glaucoma for drug delivery, minimizing its side effects with sustained release of the drug. For effective and sustain release of antiglaucoma drug. We developed two different nanoparticle chitosan and BSA nanoparticles. The size range of pilocarpine loaded BSA nanoparticle is 100 ± 16 nm, timolol maleate loaded BSA nanoparticle 50 ± 9 nm, pilocarpine loaded chitosan nanoparticle 132 ± 50 nm, and timolol maleate loaded chitosan nanoparticle 95 ± 32 nm. Following the

successful formulation of drug-loaded nanoparticles, these were incorporated into a gellan gum-based gel matrix to achieve mucoadhesive properties, sustained drug release, and to facilitate a dual drug delivery strategy. The incorporation aimed to enhance the residence time of the formulation at the ocular site and ensure prolonged therapeutic effect. Subsequently, in vitro drug release studies were conducted for both the nanoparticle suspension and the gel formulation to evaluate and compare their release kinetics. To further assess the formulation's potential for ocular application, a mucoadhesion study was performed to determine the adhesive strength of the gellan gum gel on cornea layer of the eye. Additionally, a drug permeation study was carried out using excised goat cornea as a biological membrane model, simulating transcorneal drug delivery and absorption. These evaluations were crucial in confirming the gel's efficacy in enhancing drug retention, permeation, and overall therapeutic performance.

LIST OF PUBLICATIONS

From thesis

Synthesis of nanomedicine for combating glaucoma – (manuscript under preparation)

TABLE OF CONTENTS

LIST OF FIGURES

LIST OF TABLES

NOMENCLATURE

ACRONYMS (if any)

Chapter 1:

1.1. Introduction.....	1
------------------------	---

Chapter 2:

2.1. Literature Review.....	7
2.2. Objective.....	9

Chapter 3:

3.1. Materials and Methodology.....	11
3.2. Materials.....	11
3.3. Methodology.....	11
3.3.1. Preparation of calibration curve for Pilocarpine hydrochloride..	11
3.3.2. Preparation of calibration curve for Timolol maleate.....	12
3.3.3. Synthesis of BSA nanoparticles.....	12
3.3.4. Synthesis of Pilocarpine loaded BSA nanoparticle.....	12
3.3.5. Synthesis of Timolol maleate loaded BSA nanoparticle.....	14
3.3.6. Synthesis of chitosan nanoparticle.....	14
3.3.7. Synthesis of pilocarpine loaded chitosan nanoparticle	14
3.3.8. Synthesis of timolol maleate loaded chitosan nanoparticle.....	14
3.3.9. Preparation of gellan gum solution.....	16
3.3.10. Gelation studies of gellan gum	16
3.3.11. Encapsulation efficiency.....	17
3.3.12. In-vitro drug release.....	18
3.3.13. Rheology studies of gellan gum.....	19
3.3.14. In-vitro drug release of gellan gum gel.....	20
3.3.15. Swelling index.....	20

3.3.16. In-vitro studies of cytotoxicity.....	21
3.3.17. Ex-vivo transcorneal permeation studies.....	22
3.3.18. Mucoadhesive study with flow of tear fluid.....	23
3.3.19. Evaluate the adhesive force between cornea and in-situ gel.....	23

Chapter 4:

4. Results and Discussion.....	25
4.1. Characterization of pilocarpine and timolol maleate drug.....	25
4.1.1. The absorption spectra of pilocarpine	25
4.1.2. The calibration curve of pilocarpine	25
4.1.3. The absorption spectra of timolol maleate.....	26
4.1.4. The calibration curve of timolol maleate.....	27
4.2. Characterization of BSA nanoparticle.....	29
4.2.1. Morphological analysis.....	29
4.2.2. DLS analysis.....	30
4.3. Characterization of chitosan nanoparticle	31
4.3.1. Morphological analysis.....	31
4.3.2. DLS analysis.....	33
4.4. Encapsulation efficiency of pilocarpine hydrochloride.....	33
4.5. Encapsulation efficiency of timolol maleate.....	34
4.6. In-vitro drug release studies of pilocarpine from nanoparticle.....	35
4.7. Finding optimal concentration of gellan gum.....	36
4.8. Gelation studies.....	38
4.9. Interaction between different nanoparticle with gel.....	39
4.10. Entrapment efficiency of pilocarpine and timolol maleate in gellan gum gel.....	40
4.11. In-vitro drug release studies of pilocarpine and timolol maleate in gellan gum gel.....	42
4.12. Drug release profile of dual drug.....	43
4.13. In-vitro cell toxicity by MTT analysis.....	44
4.14. Ex-vivo transcorneal permeation studies.....	45
4.15. Mucoadhesive studies.....	46

4.16. Evaluate the adhesive force between cornea and in situ gel.....	46
---	----

Chapter 5 :

5. Conclusion	49
---------------------	----

REFERENCES

LIST OF FIGURES

Figure 1: Diagrammatic representation of glaucoma	2
Figure 2: Diagrammatic representation of the synthesis of Pilocarpine-loaded BSA Nps	12
Figure 3: Diagrammatic representation of the synthesis of Pilocarpine- loaded chitosan Nps by taking different concentrations by using an ultrasonic atomizer	14
Figure 4: Schematic diagramme of gelation studies	16
Figure 5: Absorption spectra of Pilocarpine showing maximum absorbance at 215 nm	24
Figure 6: HPLC peak of Pilocarpine showing retention time at 2.927 min.....	25
Figure 7: The calibration curve of Pilocarpine having R ² value 0.9997.....	25
Figure 8: Absorption spectra of Timolol maleate showing maximum absorbance at 293 nm.....	26
Figure 9: : HPLC peak of Timolol maleate showing retention time at 2.599 min.....	26
Figure 10: The calibration curve of Timolol maleate having R ² value 0.9992.....	27
Figure 11: : SEM image of Pilocarpine loaded BSA Nps.....	28
Figure 12: SEM image of Timolol maleate loaded BSA Nps.....	28
Figure 13: Distribution curve of PLC-BSA nanoparticle.....	29
Figure 14: DLS analysis of TM BSA nanoparticles.....	29

Figure 15: Graphical representation of DLS of BSA nanoparticle.....	30
Figure16 : Graphical representation of DLS of PLC-BSA Nps.....	30
Figure 17: SEM image of Pilocarpine loaded chitosan (A & B) and Timolol Maleate loaded chitosan nanoparticles (C & D).....	31
Figure 18: Distribution curve of PLC-Chitosan nanoparticle.....	31
Figure 19: Distribution curve of TM-Chitosan nanoparticle.....	31
Figure 20: Graphical representation of DLS of PLC-chitosan nanoparticle.....	32
Figure 21: Graphical representation of drug encapsulation for Pilocarpine in BSA nanoparticles (A) and Pilocarpine in chitosan nanoparticles.....	33
Figure 22: Graphical representation of drug encapsulation for Timolol Maleate in chitosan Nps.....	34
Figure 23: <i>In vitro</i> drug release of PLC from PLC-loaded BSA.....	34
Figure 24 : In- vitro drug release of pilocarpine from chitosan Nps.....	35
Figure 25: Viscosity as a function of shear rate of different concentration of GG solution.....	36
Figure 26: Viscosity as a function of share rate of different concentration of GG solution after adding STF.....	36
Figure 27: gelation studies.....	38
Figure 28: Viscosity as a function of share rate of GG solution with different Nps.....	39

Figure 29 : Viscosity as a function of share rate of GG solution with different Nps after adding STF.....	39
Figure 30: Graphical representation of drug encapsulation for pilocarpine in Gellan gum gel.....	40
Figure 31: Graphical representation of drug encapsulation for Timilol maleate in Gellan gum gel.....	40
Figure 32: : Graphical representation of <i>In vitro</i> drug release of pilocarpine Gellan gum gel.....	41
Figure 33: Graphical representation of <i>In vitro</i> drug release of timolol maleate Gellan gum gel.....	41
Figure 34: Graphical representation of <i>In vitro</i> drug release of plc-BSA nps in Gellan gum gel.....	42
Figure 35 : Graphical representation of In vitro drug release of plc from Nps and gel.....	43
Figure 36 : The percentage of cell viability of drug loaded nanoparticle on HEK 293 cell.....	43
Figure 37 : Transcorneal permeation study of only pilocarpine hydrochloride and pilocarpine loaded in gellan gum using goat cornea.....	44
Figure 38 : Transcorneal permeation study of only pilocarpine hydrochloride and pilocarpine loaded in gellan gum using goat cornea.....	45
Figure 39 : Graphical representation of mucoadhesive test.....	46

LIST OF TABLES

Table 1. : Literature review for different particle and drug use for glaucoma.....	7
---	----------

NOMENCLATURE

Acronym	Expansion
Nps	Nanoparticles
AH	Aqueous humor
IOP	Intra ocular pressure
PLC	Pilocarpine
TM	Timolol maleate
BSA	Bovine serum albumin
TPP	Sodium triphosphate
EE	Encapsulation efficiency
STF	Simulated tear fluid
HPLC	High performance liquid chromatography
PBS	Phosphate buffer saline
GG	Gellan gum
MTT	(3-(4,5-dimethylthiazol-2-yl)-2,5 diphenyltetrazolium bromide) dye
DMSO	Dimethyl sulphoxide
FESEM	Field emission scanning electron microscopy
DLS	Dynamic light scattering

ACRONYMS

Sign	Meaning
λ	Wavelength
μ	Micron
$^{\circ}\text{C}$	Degree Centigrade
μl	Microlitre
ml	Millilitre
nm	Nanometer
$\mu\text{g/ml}$	Microgram per millilitre
mins	Minutes
hrs	Hours
R^2	Regression coefficient
%	Percentage

Chapter 1

1.1. Introduction

Eye diseases such as glaucoma represent significant concerns in adult ophthalmology, with unique causes and implications for treatment. Understanding these diseases is important for early diagnosis and effective treatment, which gives a better life for affected individuals.

Glaucoma is an eye condition that is associated with the increase in pressure of the eye referred to as IOP (intra-ocular pressure) [1]. Aqueous humor is secreted from the ciliary epithelium. If we see the cross-section of an eye, on one side of the eye we have an anterior and posterior chamber filled with the fluid called aqueous humor, and on the other side of the eye, we have a vitreous body filled with a gel-like vitreous humor [2]. In the posterior chamber, the aqueous humor is secreted by ciliary epithelium which flows to the anterior chamber through pupil. From the anterior chamber, the fluid drains out of the eye through the trabecular meshwork into the schlemm's canal and passes through the aqueous vein [3]. The controlled production and drainage of aqueous humor result in normal IOP, typically ranging from 10 mmHg – 20 mmHg [4]. In the case of glaucoma, drainage of aqueous humor is restricted, as a result, the aqueous humor builds up and exerts pressure against the vitreous body, which rises in intraocular pressure leads to damage of the optic nerve and retina [5]. Glaucoma can be defined as open-angle glaucoma and closed-angle glaucoma depending on the angle between iris and the cornea [6]. The open angle glaucoma also called wide angle glaucoma means the angle between the iris and cornea is not obstructed but the trabecular meshwork is obstructed. The closed-angle glaucoma also known as angle closure glaucoma where the angle between the iris and cornea is obstructed so the aqueous humor can't reach to the trabecular meshwork. The exact etiology of glaucoma is unknown most of the cases show a strong link between high eye pressure

and glaucoma. Increased intraocular pressure (IOP) is the primary risk factor for both the onset and progression of glaucoma [7].

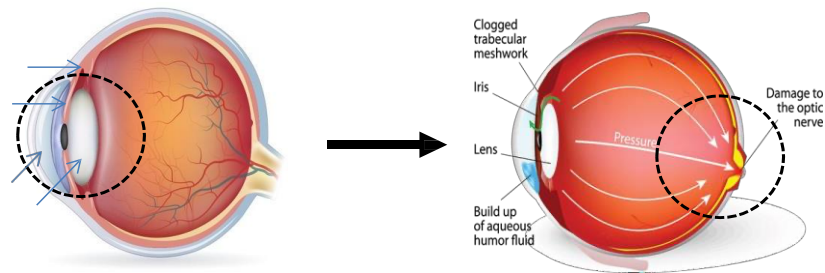


Figure 1: Diagrammatic representation of glaucoma

In current conditions there are 5 categories of commonly used antiglaucoma drugs such as prostaglandins analogs (Tafluprost, Bimatoprost, Latanoprost, Bimatoprost), beta- blockers (Timolol Maleate, Betaxolol hydrochloride, Carteolol, Levobunolol, Metoprolol), carbonic anhydrase inhibitor (Acetazolamide, Dorzolamide, Brinzolamide), adrenergic agonist (Brimonidine, Brimonidine tartrate), miotics (Pilocarpine hydrochloride) [8].

Delivering medication to the eye is difficult due to several barriers. In-situ gelling systems, applied topically, are increasingly popular in ocular treatments. These systems offer a promising way to improve how we treat various eye conditions. The eye is very good at protecting itself, which makes it difficult for medications delivered as eye drops to be absorbed effectively. Several natural defenses and other factors limit how well drugs can enter the eye. These include the eye's drainage system, tear production, metabolism, and the way drugs interact with eye tissues. Also, only a small area of the cornea is available for absorption,

and it doesn't let drugs pass through easily when you put in eye drops, the eye can only hold a tiny amount of fluid (7–10 μL). Since a typical eye drop is much larger (50–100 μL), the extra liquid quickly drains away through the tear ducts into the nose and stomach, carrying the drug with it. As a result, the medicine only stays in contact with the cornea and sclera (the parts of the eye that absorb it) for a very short time, about 2 minutes at most.

The biggest problem with delivering drugs to the eye is making sure the right amount of medication gets to where it needs to be and stays there long enough to work. Sometimes, the medication that drains through the tear duct ends up being absorbed into the rest of the body, which can lead to unwanted side effects. This is because the drug is not just acting on the eye, but is also entering the bloodstream and affecting other parts of the body. To tackle these issues, scientists have been exploring different ways to deliver eye medications. They've looked at options like suspensions, ointments, inserts, and special gels that are designed to keep the drug in contact with the eye for a longer period. The goal is to help the medication stay in the eye longer so it can be more effective. While these alternative methods are better than standard eye drops, they come with their own problems. Ointments can blur your vision, and things like eye inserts can be uncomfortable or difficult to use, so people don't always stick with them. Because of these issues, it's still difficult to get enough of a drug absorbed into the eye when applying it topically. Finding a way to effectively deliver medication through eye drops remains a significant challenge. Using ready-made gels for eye medication has its drawbacks, which limits how often they're used. It's hard to measure out the right dose consistently with these gels. Plus, they can cause blurry vision, crusty eyelids, and excessive tearing after you put them in. A newer approach is the in-situ gel system, which mixes the best parts of gels and liquid solutions. This way, you can easily and accurately apply the medication. These special formulations start as a liquid before you use them, but they turn into a gel once they're inside

your eye. In-situ gelling delivery systems hold great promise as an effective way to administer eye medications. Applying them in liquid form makes it easy, safe, and consistent to administer. Additionally, they are easier to prepare and manufacture on a large scale compared to traditional solid or semi-solid medications.

The key innovation of these smart hydrogels lies in their ability to transform from a solution to a gel when triggered by conditions found on the eye's surface, such as temperature, pH, or ionic strength. Once applied, these hydrogels quickly turn into a gel, which helps them stay on the eye longer by reducing pre-corneal elimination. Using biopolymers with mucoadhesive properties further enhances how long these gels stay on the eye's surface. This extended contact time increases the absorption of the active ingredients, leading to better bioavailability and improved effectiveness. Furthermore, reducing pre-corneal elimination also decreases systemic absorption, which can minimize side effects. Overall, ophthalmic in-situ gelling systems offer a promising approach to improve the treatment of anterior eye conditions and can be seen as a novel strategy for formulating medications with poor ocular absorption

Gellan gum, discovered in 1978, is a special type of substance made by *Sphingomonas paucimobilis* bacteria. It's built from a repeating unit containing rhamnose, glucuronic acid, and glucose. When gellan gum forms a gel, it starts by creating tiny, twisted structures that then link up with each other. This process is helped along by charged particles called cations and by water molecules, which together build a 3D network that gives the gel its shape. How well gellan gum forms a gel depends on the type of cations present. Divalent cations, which have a stronger positive charge, are much better at promoting gel formation compared to monovalent cations, which have a weaker positive charge[9]. Gellan gum mixtures turn into a gel because of the presence of ions like sodium,

potassium, magnesium, and calcium in tear fluid[10]. Gellan gum's special properties make it a common choice in medicines, helping drugs stay stable and work effectively. However, regular gellan gum isn't suitable for eye-related uses because it's too heavy, uneven in its makeup, and doesn't dissolve well in pure water, leading to cloudy solutions. For instance, to dissolve regular gellan gum, you need to heat it under specific conditions [11]. A type of gellan gum with low acyl content deacylated gellan gum is used as a gelling agent because it creates gels that are clear, strong, and stable across a wide range of pH. This particular type of gellan gum was selected for its ability to form gels when it comes into contact with positively charged ions [12]. Using low acyl gellan gum to create gels directly in the body has shown promising results. The gels formed are clear, strong, stable, and soft, and these qualities have led to positive outcomes in both laboratory and clinical trials [13]. Gellan gum is one of the most promising *in situ* gelling polymers in the human body and applicable for biomedicine technology, such as drug delivery vehicles

Various types of nanoparticles are used in drug delivery for glaucoma. Nanoparticles can be classified into different categories such as polymeric nanoparticles, protein-based nanoparticles, liposomal nanoparticles, quantum dots, etc [14]. A natural polymer chitosan and bovine serum albumin is used to prepare drug delivery vehicles. Chitosan helps to increase drug permeability and increase corneal penetration and in the case of ocular drug delivery BSA nanoparticle was also helpful because BSA degrades in contact with lysozyme which is present in tear fluid as an antimicrobial agent. Chitosan has a positive charge so due to electrostatic interaction chitosan binds with a negatively charged corneal layer [15]. Among polymeric nanoparticles chitosan nanoparticles gaining importance because of being efficient, cost-effective, and environmentally friendly [16].

In this study, we have developed a drug-loaded nanoparticle system incorporated into an ion-activated in situ gel to achieve sustained drug release. The use of the in situ gel formulation aims to minimize drug loss, which typically occurs due to tear fluid secretion and eye blinking, thereby enhancing the retention time of the drug in the ocular region.

Common route for nanomedicine administration in eye are Eyedrops, intracameral injection (in the cornea or anterior chamber), intravitreal injection (directly in vitreous humor), subconjunctival injection, and intravenous injection

Chapter 2

2.1. Literature Review

Table 1: Literature review for different particle and drug use for glaucoma

Sl	Particle	Drug	Objective	Reference
1	Gelatine core liposome	TM	Synthesis of TM-loaded gelatin core liposome and target glaucoma for reducing the intraocular pressure	[17]
2	Liposome-incorporated ion-sensitive in situ gel	TM	Aimed to design liposome-based ion- sensitive in situ gel for delivering Timolol Maleate to reduce the IOP	[18]
3	Galactosylated chitosan Nps	TM	Aim to formulate nanoparticles made from galactosylated chitosan loaded with Timolol, used to treat glaucoma, and evaluate the effectiveness of these nanoparticles as a delivery system for ocular applications.	[19]

4	Chitosan sodium alginate Nps	TM	Development of Nanogel-based natural polymers as smart carriers for the controlled delivery of Timolol Maleate through the cornea for glaucoma	[20]
5	PLGA nanoparticle	Brinzolamide	Synthesis of PLGA nanoparticles as subconjunctival injection for management of glaucoma	[21]
6	Chitosan pectin mucoadhesive nanocapsule	Brinzolamide	Formulate chitosan pectin mucoadhesive nanocapsule loaded with brinzolamide for the management of glaucoma	[22]

2.2. Objective

The aim is to construct an *in-situ* gel having Pilocarpine and Timolol Maleate drugs loaded in BSA and chitosan nanoparticles for the treatment of glaucoma, for improved encapsulation, permeation and release profile of drug.

Chapter 3

3.1. Materials and Methodology

3.2. Materials:

Chitosan (SRL chemicals), Sodium Tripolyphosphate - TPP (Sigma Aldrich), Pilocarpine hydrochloride (Sigma Aldrich), Ethanol, Glacial acetic acid, Bovine Serum Albumin, Timolol Maleate eye drops IP (SUN pharmaceuticals), Glutaraldehyde (spectrochem), Gelrite Gellan Gum (SRL chemicals), Sodium chloride (Himedia), Sodium bicarbonate (Rankem), Calcium Chloride Dihydrate (SRL Chemicals)

3.3. Methodology

3.3.1. Preparation of calibration curve for Pilocarpine drug

First, we prepare the calibration curve of Pilocarpine Hydrochloride that gives the regression equation and linearity coefficient. Preparation of calibration curve for Pilocarpine by dissolving the drug in distilled water followed by making different concentrations 25µg, 50µg, 75µg, 100µg, 125µg, 150µg, 175µg and 200µg. Then we plot the calibration curve using the High- performance liquid chromatography method using acetonitrile: potassium dihydrogen phosphate buffer (60:40) with 1ml/min flow rate as a mobile phase.

3.3.2. Preparation of calibration curve of Timolol Maleate drug

Similarly, we prepare the calibration curve of Timolol maleate using High- performance liquid chromatography, which provides the regression equation and linearity coefficient. Preparation of calibration curve for Timolol Maleate by making different concentrations 10 µg, 20 µg, 30 µg, 40 µg, 50 µg, 60 µg, 70 µg 80 µg, 90 µg and 100 µg. Then we plot the calibration curve using the High- performance liquid chromatography method using acetonitrile: potassium dihydrogen phosphate buffer (60:40) with 1ml/min flow rate as a mobile phase.

3.3.3. Synthesis of Bovine serum albumin (BSA) nanoparticles

To synthesize the BSA nanoparticle, we used 100 mg of BSA in 5 mL Milli-Q water with approx. 7.4 pH value, then stirred at 650 rotation per minute at room temperature for 5 minutes. Then, the conversion of the dissolved protein into a protein nanoparticle through continuous 100% ethanol addition at the rate of 1 mL/min, the process was carried out until the turbidity was observed. After 5 minutes, the reaction was kept under constant magnetic stirring for 12 hours by adding 100 µl of 8% aqueous glutaraldehyde (v/v) as a cross-linker to cross-link the BSA nanoparticles. Then purification of the suspension was performed by three cycles of centrifugation at 30,000 g for 20 minutes to remove non-dissolved protein, ethanol, and glutaraldehyde. At each centrifugation cycle, nanoparticles were redispersed in 10 ml of deionized water and followed by using ultrasonication bath for 5 minutes. To get nanosized BSA particles.

3.3.4. Synthesis of pilocarpine loaded BSA nanoparticle

To synthesize pilocarpine loaded BSA nanoparticle , we used 2% of BSA solution with different concentration of pilocarpine 1mg/ml and 0.5 mg/ml, then stirred at 650 rotation per minute at room temperature for 5 minutes. . Then, the conversion of the dissolved protein with the

drug into drug-loaded nanoparticles through continuous 100% ethanol addition at 1 ml/min the process was carried out until the turbidity was observed. After 5 minutes, the reaction was kept under constant magnetic stirring for 12 hours by adding 100 μ l of 8% aqueous glutaraldehyde (v/v), as a cross-linker to cross-link the drug-loaded protein nanoparticles. . Then purification of suspension was performed by three cycles of centrifugation at 30,000 g for 20 minutes to remove ethanol, non-dissolved BSA, and glutaraldehyde. At each centrifugation cycle, nanoparticles were redispersed in 10 ml of deionized water and followed by using ultrasonication bath for 5 minutes. To get nanosized Pilocarpine loaded BSA nanoparticle.

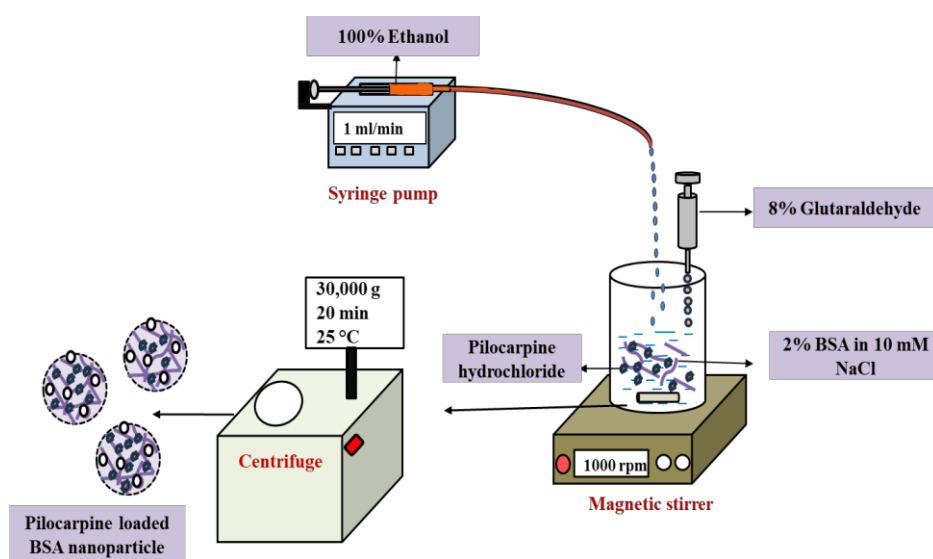


Figure 2: Diagrammatic representation of synthesis of Pilocarpine loaded BSA nanoparticles

3.3.5. Synthesis of Timolol Maleate-loaded BSA nanoparticle

Similarly, to synthesize Timolol Maleate loaded BSA nanoparticle, we used 2% of BSA solution with a concentration of Timolol Maleate 0.5 mg/ml, then stirred at 650 rotation per minute at room temperature for 10 minutes. Then conversion of the dissolved protein with the drug into drug-loaded nanoparticles through continuous 100% ethanol addition at 1 ml/min and this process was continued until the solution was turbid. After 5 minutes, the reaction was kept under constant magnetic stirring for 12 hours by adding 100 μ l of 8% aqueous glutaraldehyde (v/v), as a cross-linker to cross-link the BSA nanoparticles. Then purification of suspension was performed by three cycles of centrifugation at 30,000 g for 20 minutes to remove glutaraldehyde, non-dissolved BSA, and ethanol. At each centrifugation cycle, nanoparticles were redispersed in 10 ml of deionized water and followed by using ultrasonication bath for 5 minutes. To get nanosized powder of Timolol Maleate loaded BSA nanoparticle.

3.3.6. Synthesis of chitosan nanoparticles

The formation of chitosan nanoparticles was done using the ultrasonic atomizer. In a syringe, the sample of 0.5% (w/v) of chitosan was taken whereas 50 ml of 1% (w/v) sodium tripolyphosphate was taken in a beaker and placed below the nozzle of the atomizer on a magnetic stirrer at 1500 rpm. The chitosan solution loaded on the syringe was pumped and sprayed with a 0.3 ml/min flow rate at a frequency of 130 kHz, and power of 3.5 watts. The sprayed droplets were collected in 1% sodium tripolyphosphate (TPP) acting as a cross-linker[23]. The nanosuspension was centrifuged at a speed of 30,000 g for 15 mins at 25 °C. The supernatant was collected and washed the pellet three times with 20 ml distilled water. The pellet was stored at 4 °C for further analysis.

3.3.7. Synthesis of Pilocarpine-loaded chitosan nanoparticle

Similarly, the Pilocarpine-loaded chitosan nanoparticles were synthesized using an ultrasonic atomizer. In a syringe, 0.5% (w/v) of 1 ml chitosan was taken with different concentrations of Pilocarpine such as 0.5 mg/ml, and 1 mg/ml. Then 1% (w/v) TPP (50 ml) was taken in a beaker on a magnetic stirrer for stirring at 1500 rpm. Then different samples of the drug and chitosan were sprayed and collected in TPP. The nanosuspension was collected and centrifuged followed by the washing step with distilled water. Both the supernatant and pellet were collected to calculate the encapsulation efficiency and characterization.

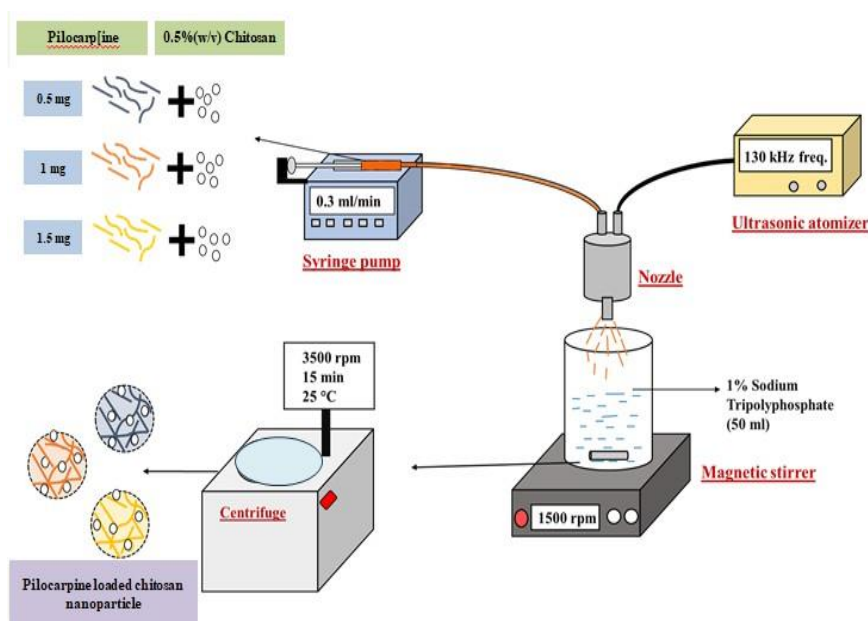


Figure 3: Diagrammatic representation of the synthesis of P L C - loaded chitosan nanoparticles by using an ultrasonic atomizer

3.3.8. Synthesis of Timolol Maleate-loaded chitosan nanoparticle

Similarly, the Timolol Maleate-loaded chitosan nanoparticles were synthesized using an ultrasonic atomizer. In a syringe, 0.5% (w/v) of 1 ml chitosan was taken with different concentrations of Timolol Maleate such as 0.5 mg/ml, 1 mg/ml, and 1.5 mg/ml. Then 1% (w/v) TPP (50 ml)

was taken in a beaker and put on a magnetic stirrer for stirring at 1500 rpm. Then different samples of the drug and chitosan were sprayed and collected in TPP. The nanosuspension was collected and centrifuged followed by the washing step with distilled water. Both the supernatant and pellet were collected to calculate the encapsulation efficiency and characterization.

3.3.9. Preparation of Gellan gum solution

To develop an effective formulation, placebo in-situ gelling systems were created with different different polymer, and assessed for their gelling capabilities to determine the optimal concentration. Gellan gum was dissolved in ultrapure water by heating the solution to 70–80°C while stirring. To evaluate gelling capacity, a drop of each system was introduced into a vial containing 2 mL of simulated tear fluid (STF), which was freshly prepared. The STF composition included 0.670 g of sodium chloride, 0.200 g of sodium bicarbonate, 0.008 g of calcium chloride dihydrate, and sufficient purified water to bring the total weight to 100 g, following the formulation by. Rozier et al. (1989). [F]

3.3.10. Gelation studies

In this study, we aim to investigate whether the gelation of gellan gum is sensitive to pH or ion concentration. To achieve this, we prepared 10 mL aliquots of different pH buffer solutions, which included pH 4, pH 6, pH 7, pH 9, simulated tear fluid, and distilled water, each contained in separate glass bottles. Subsequently, 1 mL of a 0.25% (w/v) gellan gum solution was added to each of the buffer solutions. Since gellan gum is naturally transparent, methylene blue dye was incorporated to aid in the visualization of gel formation. The gelation behavior was then observed and analyzed to determine the influence of pH and ionic conditions on the gel's properties.

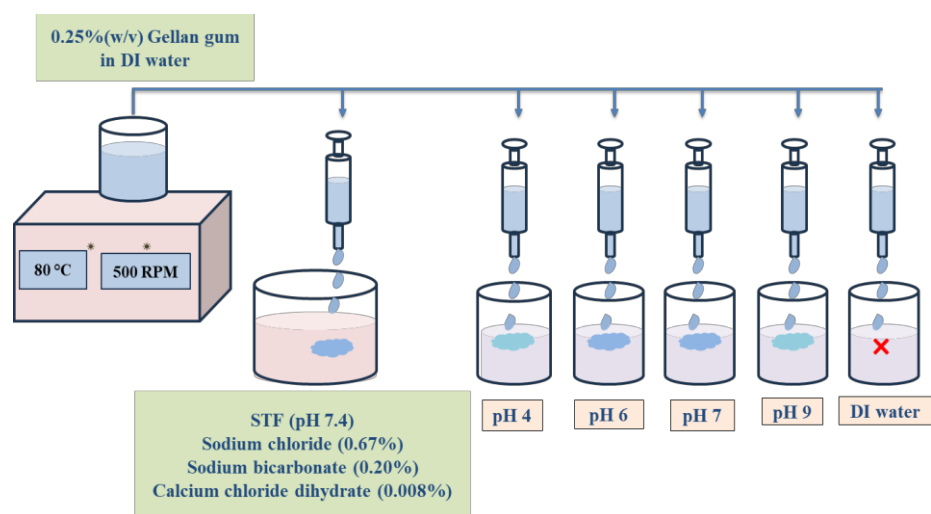


Figure 4: Schematic diagramme of gelation studies

3.3.11. Encapsulation Efficiency

The encapsulation efficiency is used to determine the percentage or amount of drug encapsulating inside the nanoparticles successfully. There are 2 different methods of calculating EE- direct and indirect method.

Direct method – in this method, we calculate the amount of drug encapsulating by breaking the nanoparticles. The pellet of chitosan nanoparticles was dissolved in 50% acetic acid and left for 6-10 hours with a constant stirring at 50 rpm. Then the sample was centrifuged at 12,000g to remove the chitosan and the supernatant was collected because it contained the amount of drug that was encapsulated in chitosan nanoparticles. The absorbance was measured at a characteristic wavelength of the drug.

$$\text{Encapsulation efficiency (\%)} = (A1 / A0) \times 100$$

A0 - Initial drug loaded, A1 - Amount of drug encapsulated in Nps, A2 - Amount of drug left in the supernatant

Indirect method - Here, we analyzed the supernatant collected during the initial formulation of the nanoparticles. In this, the supernatant has the amount of drug that was not encapsulated inside the nanoparticles. The absorbance of the UV-visible spectrophotometer was measured to determine the concentration of the loaded drug inside the nanoparticles by applying the formula given below.

$$\text{Encapsulation efficiency (\%)} = (A_0 - A_2 / A_0) \times 100$$

A₀ - Initial drug loaded, A₁ - Amount of drug encapsulated in Nps, A₂ - Amount of drug left in the supernatant

In case of gel, preparation and evaluation of drug-loaded gellan gum gel, a specific amount of the drug was first incorporated into the gellan gum solution to ensure homogeneous dispersion. The drug-loaded gellan gum solution was then mixed with simulated tear fluid (STF), which contains ionic components that facilitate the gelation process through ionic crosslinking. This transition from solution to gel mimics the in situ gelation that occurs upon instillation into the eye.

To assess the remaining quantity of the drug in gel, the excess simulated tear fluid was collected after gel formation. The collected STF was subsequently analyzed using high-performance liquid chromatography (HPLC) to quantify the amount of drug released into the surrounding medium. This methodology allowed us to determine the drug loading in the gellan gum gel.

3.3.12. *In vitro* drug release

We perform *In vitro*, drug release as a study to measure the amount of drug released from the different nanoparticles at periodic time intervals. This *in-vitro* study was done with the help of a dialysis membrane bag and 80 ml of PBS with a pH value of 7.4. The drug-loaded nanoparticle was suspended with 3 ml of PBS and enclosed into a dialysis bag each

having 1 ml of resuspended nanoparticles and kept on a magnetic stirrer at 200 rpm and 37 °C. Then 1 ml of sample was withdrawn at different time intervals by replacing the same amount of fresh PBS. The readings of the withdrawn samples were taken using high-performance liquid chromatography and UV-vis spectrophotometer for 6 hrs. After that, the percentage of drug release was calculated at a different time.

3.3.13. Rheology studies of Gel

Anton Paar rheometer (Physica MCR 301) was used to determine the viscosity of 0.25%, 0.5%, and 0.75% (w/v) GG solutions. When it contact with tear fluid then how much change in viscosity also measured. The setup for measuring viscosity involves a vertical probe. This probe touches the sample, which is placed on a flat, horizontal plate. As the probe interacts with the sample, it determines the sample's viscosity. For each concentration of gellan gum solution (0.25%, 0.5%, and 0.75% w/v), one milliliter was carefully positioned under the rheometer's vertical probe. The viscosity was then assessed across 30 different shear rates. The temperature was maintained at 25 ± 0.5 °C throughout the measurements to ensure consistent conditions. We also studies BSA nanoparticle and chitosan nanoparticle with gellan gum solution and also with tear fluid to check the change in viscosity. In this study we check the introduction of BSA nanoparticle and chitosan can change in viscosity of gellan gum or not. The goal was to find a gellan gum concentration that provides the best viscosity both before and after contact with tear fluid. This ensures it flows well and gels effectively. The study focused on observing how different concentrations of gellan gum change in viscosity to determine the ideal viscosity for the formulation.

3.3.14. *In-vitro* drug release of gellan gum gel

In-vitro drug release was studied using a magnetic stirring method. A dialysis bag containing 1 ml of gellan gum gel with nanoparticle and two drug, timolol maleate was in gellan gum solution and pilocarpine was encapsulate in BSA nanoparticle was placed in 80 ml of artificial tear fluid as the external medium. This setup allowed for the assessment of how the drug is released from the formulations into the artificial tear fluid. The use of a dialysis bag ensures that only the dissolved drug can pass through, mimicking the *in vivo* conditions where the drug needs to be in solution to be absorbed. The magnetic stirring ensures uniform distribution and consistent drug diffusion from the dialysis bag into the surrounding fluid, which is crucial for accurate and reproducible results. Drug release was monitored over a 10-hour period with samples taken at specific intervals: 10, 20, 30, 40, 50 minutes, then at 1, 2, 4, 8, and 10 hours. These samples were analyzed using HPLC to quantify the amount of dissolved drug at each time point. The concentration of the drug in solution was measured at each time point using HPLC (High-Performance Liquid Chromatography). This method allows for accurate determination of the amount of drug released from the formulations over time. Finally, a graph was generated to show the percentage of cumulative drug release against time. This graph provides a visual representation of the drug release profile, illustrating how the drug is released from the formulation over the 10-hour period.

3.3.15. Swelling index

In this study we check the gellan gum gel swell or not after gel formation in the presence of artificial tear fluid. At first we take 6 number of 1 ml of 0.25%(w/v) gellan gum solution and weigh the solution before adding artificial tear fluid. And then we add artificial tear fluid in all six MCT at 0 sec then we weigh the gell at different time interval from different

different MCT after removing the extra artificial tear fluid , then we measure the change in weight of these gellan gum gel The water uptake capacity of gel was assessed by determining their swelling index. A precise mass of 900 mg of the thin films was immersed in 3 ml of simulated tear fluid (pH 7.4) separately. The immersion was conducted in a disc and maintained at a temperature of 37 °C for a duration of 30 minutes. Following this period, the excess tear fluid solution was carefully removed from the surface of the gel using tissue paper to blot them dry. The weight of the swollen gel was then immediately recorded. To ensure the reliability of the results, each experiment was performed three times.

The swelling index, which indicates the degree of swelling, was calculated using a specific formula. This calculation reflects the percentage of water absorbed by the gellan gum gel under the given conditions.

Swelling index = (weight of swollen thin films–intial weight of thin film)/ initial weight of thin film * 100

3.3.16. *In-vitro* study of cytotoxicity

To evaluate the cytotoxic effects of the synthesized BSA nanoparticle, an MTT assay was conducted. Healthy kidney cells (HEK 293) was plated in 96-well plates at a density of 10,000 cells per well and allowed to grow until they reached confluency. The cells were then exposed to the nanoparticle and incubated for 48 hours. After this incubation period, 200 µl of MTT solution was added to each well, and the plates were further incubated for 3 hours to allow the metabolically active cells to convert the yellow MTT into insoluble purple formazan crystals. Following this, 100 µl of DMSO was introduced to dissolve the formazan crystals, and the absorbance was read at 570 nm using a microplate reader. The cell viability was determined by comparing the absorbance of treated cells to that of untreated control cells, expressed as a percentage.

3.3.17. *Ex-vivo* transcorneal permeation study

Whole goat eyeballs were obtained from a nearby slaughterhouse and promptly transported to the laboratory under refrigerated conditions using normal saline to maintain tissue viability. The corneas were meticulously excised alongside a 10 to 20 mm margin of the adjacent scleral tissue to ensure structural integrity. These isolated corneas were then preserved in freshly prepared simulated tear fluid (STF) at a physiological pH of 7.4 to mimic the natural ocular environment. This preparation of goat corneas served as the biological membrane for investigating the transcorneal permeation characteristics of pilocarpine and timolol maleate from the newly developed ophthalmic formulation.

The experiment was conducted using a modified Franz diffusion chamber comprising six individual cells, each consisting of an upper and lower compartment. The upper chamber functioned as the donor compartment, where the drug solution or formulation being tested was placed. A freshly excised goat cornea separated the upper and lower chambers, acting as the permeation barrier. The lower chamber, known as the receiver compartment, was filled with simulated tear fluid (STF) to mimic the natural ocular environment. The entire system was carefully maintained at a constant temperature of $37 \pm 0.5^{\circ}\text{C}$ to simulate physiological conditions. Samples of the fluid from the receiver compartment were collected at regular intervals over a period of six hours using pre-weighed microcentrifuge tubes. These samples were then analyzed using a validated HPLC method to measure the concentrations of pilocarpine and timolol maleate. After the completion of the permeation study, the remaining drug in the donor compartment was also collected and quantified with HPLC, allowing for calculation of the total amount of drug that had permeated through the cornea.

3.3.18. Mucoadhesive study with tear fluid flow

A mucoadhesive test was conducted to evaluate the adhesive force between the cornea and gellan gum gel. In this experiment, the eyeball of a goat was fixed in position, and gellan gum solution was applied onto the corneal surface. To enable visualization of the otherwise transparent gellan gum, methylene blue dye was incorporated into the gel formulation prior to application. Subsequently, simulated tear fluid was continuously flowed over the corneal surface at a rate of 300 $\mu\text{L}/\text{min}$ for a duration of 2 hours. The retention of the gellan gum gel on the cornea was then assessed to determine its mucoadhesive properties under dynamic tear flow conditions.

3.3.19. Mucoadhesive study to check the adhesion force between cornea and in situ gel

In a separate experiment, a mucoadhesive strength test was conducted using a blink force simulation setup. The apparatus was designed with two excised corneal tissues arranged in a vertical orientation: one cornea was fixed to the lower platform and the other to the upper platform. A sample of gellan gum gel was placed between the two corneal surfaces to simulate ocular application. To evaluate the adhesive strength, incremental weights were applied to the upper platform until the detachment of the corneal tissues occurred. The maximum weight sustained without separation was recorded as a measure of the mucoadhesive strength of the gellan gum gel.

Chapter 4

4. Result and Discussion

4.1. Characterization of Pilocarpine hydrochloride and Timolol maleate drug

4.1.1. The absorption spectra of Pilocarpine Hydrochloride

When the absorbance of Pilocarpine was taken using a UV- vis spectrophotometer, a broad spectrum was obtained from 190 nm to 240 nm and the maximum absorbance was measured at 215 nm.

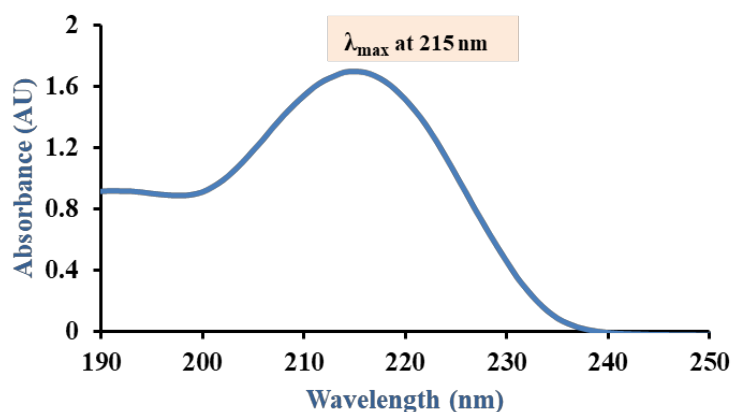


Figure 5: Absorption spectra of Pilocarpine showing maximum absorbance at 215 nm

4.1.2. The calibration curve of Pilocarpine hydrochloride

The calibration curve of the Pilocarpine drug was made by making different concentrations of the drug in distilled water. Then we plot the calibration curve using the High-performance liquid chromatography method using acetonitrile: 10 mM potassium dihydrogen phosphate buffer (60:40) (v/v) as a mobile phase with 1ml/min flow rate. which provides the linearity coefficient 0.9997 and regression equation $y = 30001x - 12707$.

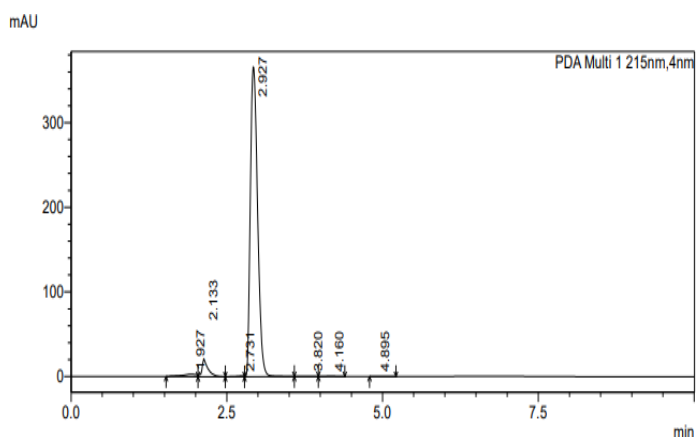


Figure 6: HPLC peak of PLC showing retention time at 2.927 min

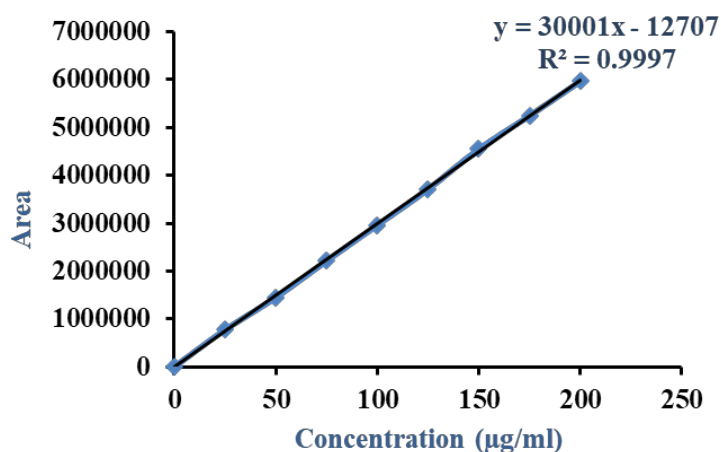


Figure 7: The calibration curve of PLC having R^2 value 0.9997

4.1.3. The absorption spectra of Timolol Maleate

When the absorbance of Timolol Maleate was taken using a UV-vis spectrophotometer, a broad spectrum was obtained from 260 nm to 360 nm and the maximum absorbance was measured at 293 nm.

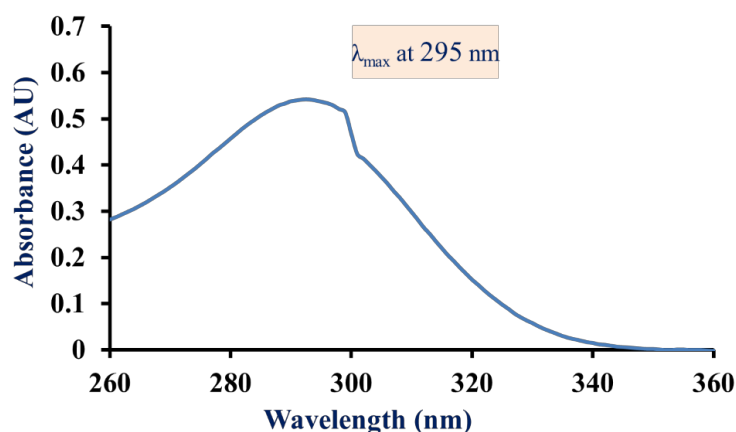


Figure 8: Absorption spectra of Timolol Maleate showing maximum absorbance at 293 nm

4.1.4. Calibration curve of Timolol Maleate

The calibration curve of the Timolol maleate drug was made by making different concentrations of the drug in distilled water. Then we plot the calibration curve using the High-performance liquid chromatography method using acetonitrile: 10 mM potassium dihydrogen phosphate buffer (60:40) (v/v) as a mobile phase with 1ml/min flow rate. which provides the linearity coefficient 0.9981 and regression equation $y = 30719x - 9654.5$

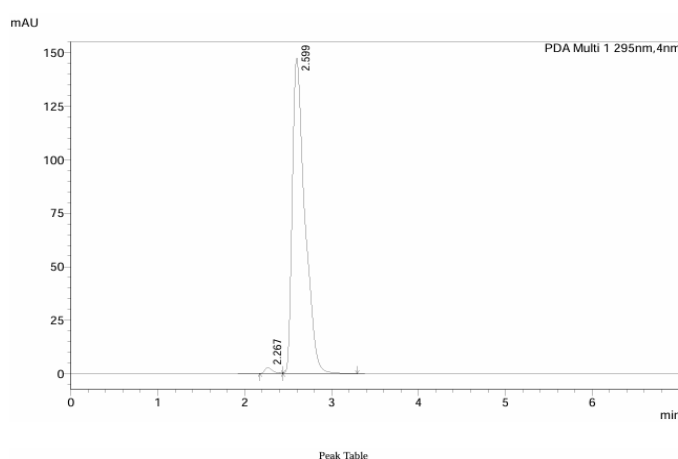


Figure 9: HPLC peak of Timolol maleate showing retention time at 2.599 min

The calibration curve of the drug, Timolol Maleate was made by taking different concentrations of the drug in distilled water. Then we measure the absorbance of a given concentration using a UV-visible spectrophotometer. This UV-visible spectrophotometer works on the principle of Beer's Lambert law. This law states that the absorbance and concentration are directly proportional to each other. The calibration curve of Timolol Maleate was plotted and the regression equation and R^2 value were calculated. The regression equation obtained was $Y = 0.0271X - 0.0261$ and the linearity coefficient (R^2) value was 0.9992 which was near 1. This equation will be used for further calculation of the drug and its encapsulation efficiency

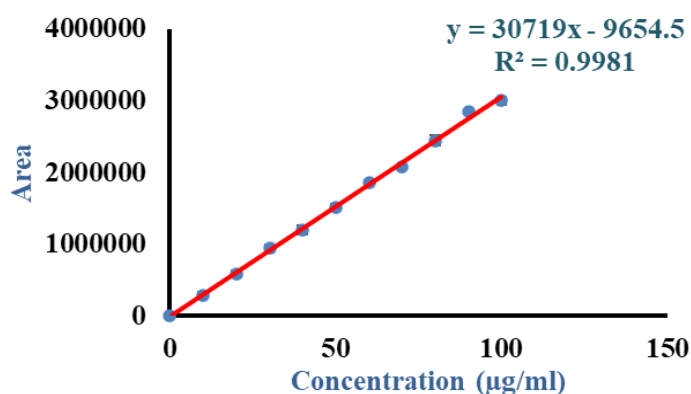


Figure 10: The calibration curve of Timolol having R^2 value 0.9981

4.2. Characterization of BSA nanoparticle

4.2.1. Morphological analysis

The size and shape of BSA nanoparticles were analyzed using field emission scanning electron microscopy. The BSA nanoparticle was spherical and uniform in size and shape. The size of Pilocarpine-loaded BSA nanoparticle was calculated and found to be 100 ± 16 nm and the size of a Timolol Maleate-loaded BSA nanoparticle was found to be 50 ± 9 nm

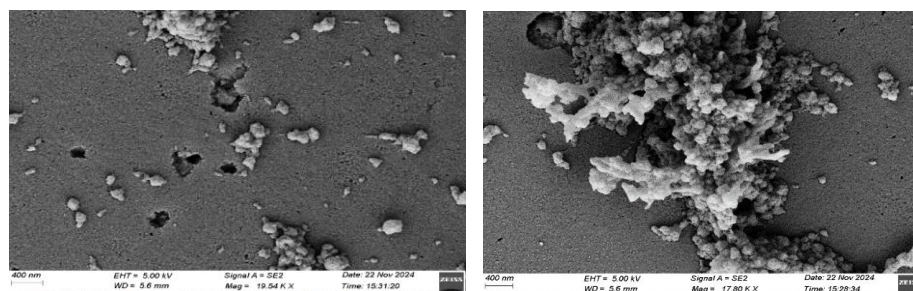


Figure 11: SEM image of Pilocarpine loaded BSA Nps

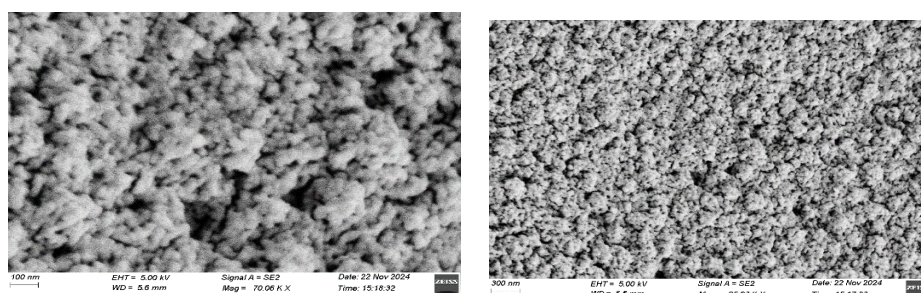


Figure 12: SEM image of Timolol Maleate loaded BSA Nps

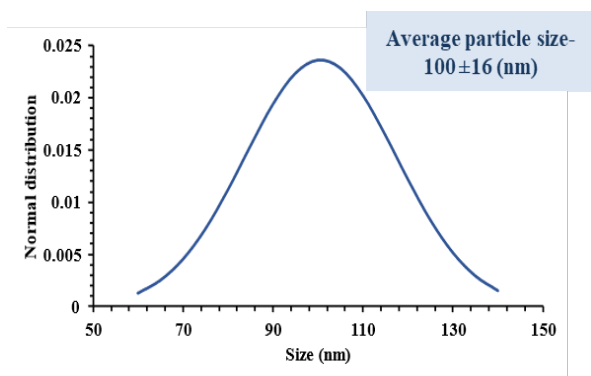


Figure 13: Distribution curve of PLC-BSA nanoparticle

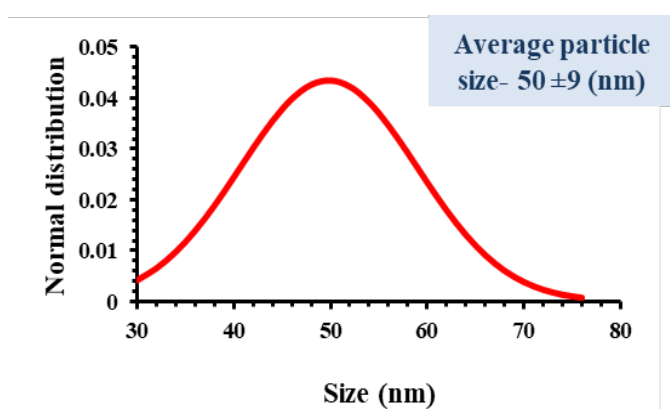


Figure 14: Distribution curve of TM BSA nanoparticles

4.2.2. DLS Analysis

The size of BSA nanoparticles was analyzed by DLS. The BSA nanoparticle was uniform in size. The size of the BSA nanoparticle was calculated and found to be 176 ± 58 nm

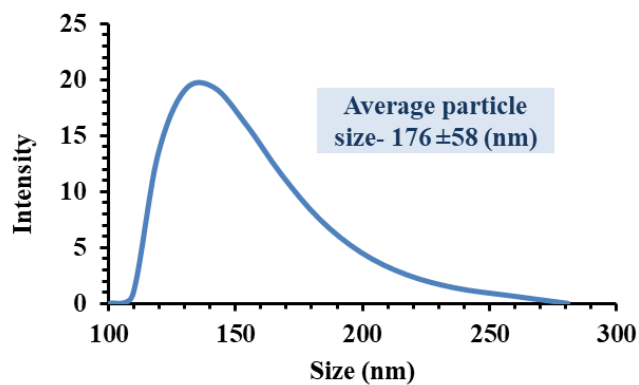


Figure 15 : Graphical representation of DLS of BSA nanoparticle

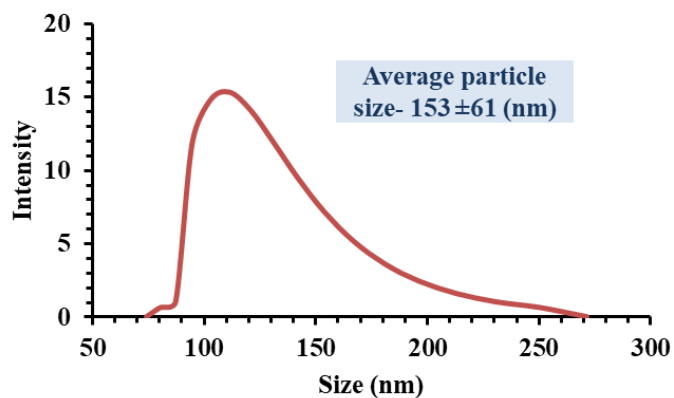


Figure 16 : Graphical representation of DLS of PLC-BSA Nps

4.3. Characterization of chitosan nanoparticle

4.3.1. Morphological analysis

The size and shape of chitosan nanoparticles were analyzed by FESEM. The chitosan nanoparticle was spherical and uniform in size. The size of the Pilocarpine-loaded chitosan nanoparticle was calculated and found to be 132 ± 50 nm and the size of the Timolol Maleate-loaded chitosan nanoparticle was found to be 95 ± 32 nm.

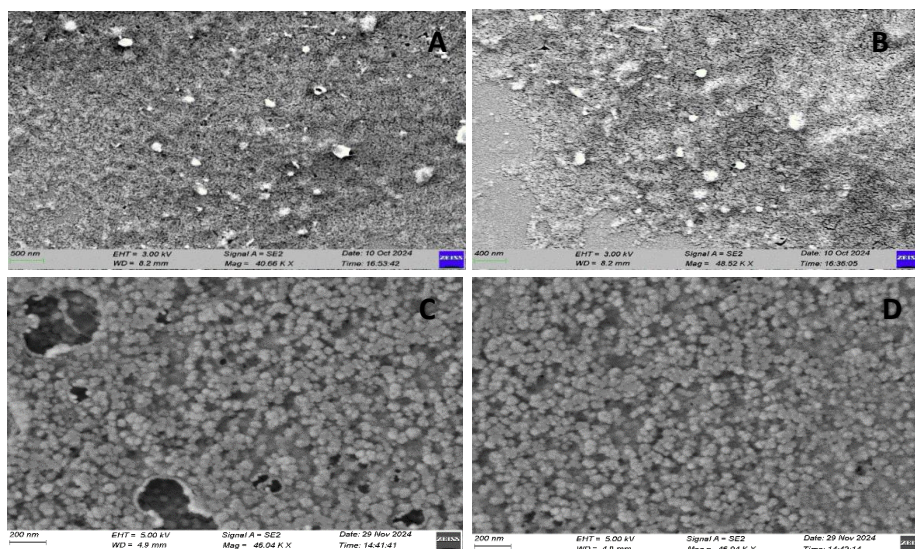


Figure 17: SEM image of Pilocarpine loaded chitosan (A & B) and Timolol Maleate loaded chitosan nanoparticles (C & D)

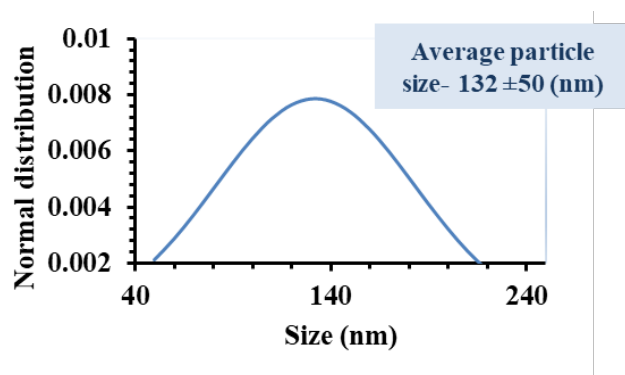


Figure 18 : Distribution curve of PLC-Chitosan nanoparticle

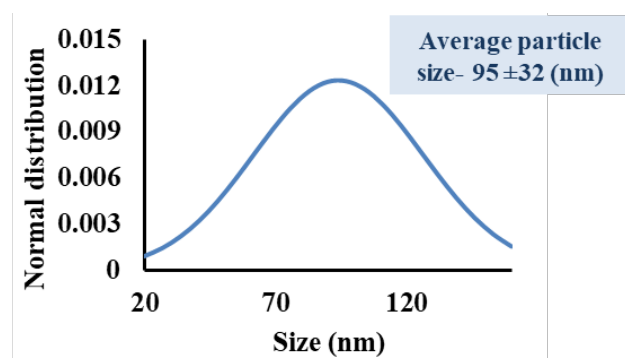


Figure 19 : Distribution curve of TM-Chitosan nanoparticle

4.3.2. DLS analysis

The size of Chitosan nanoparticles was analyzed by DLS. The chitosan nanoparticle was uniform in size. The size of the Pilocarpine-loaded chitosan nanoparticle was calculated and found to be 183 ± 66 nm

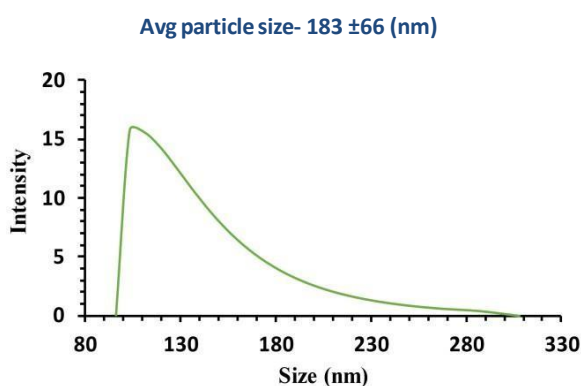


Figure 20: DLS graph of PLC-chitosan nanoparticle

4.4. Encapsulation Efficiency of Pilocarpine hydrochloride

The encapsulation efficiency of Pilocarpine was calculated in different nanoparticles and optimized by taking 0.5 mg/ml, and 1 mg/ml drug in BSA nanoparticles and 1 mg/ml, 1.5 mg/ml in chitosan nanoparticles. The % of encapsulation efficiency of Pilocarpine was calculated. When we took 1 mg /ml of the drug the maximum encapsulation efficiency was found as 22 % in the case of BSA nanoparticle.

In the case of chitosan 1 mg/ml, the maximum encapsulation efficiency was calculated at 20.6%

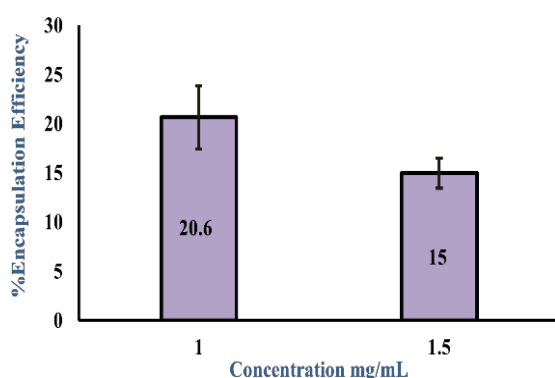
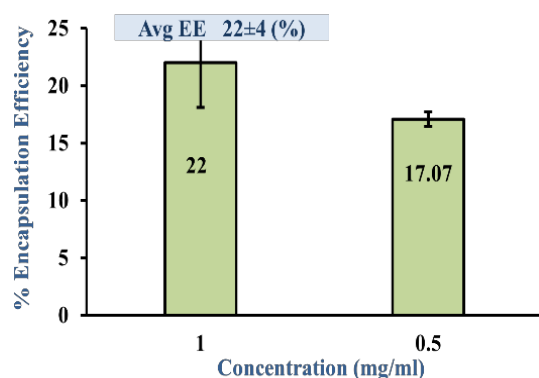


Figure 21: Drug encapsulation for Pilocarpine in BSA nanoparticles (A) and Pilocarpine in chitosan nanoparticles (B)

4.5. Encapsulation Efficiency of Timolol Maleate

The encapsulation efficiency of Timolol Maleate was optimized by taking 1 mg/ml, 1.5 mg/ml and 2 mg/ml drug in chitosan nanoparticles. The % of encapsulation efficiency of Timolol Maleate was calculated. When we took 1 mg /ml of the drug the encapsulation efficiency was found as 19.7 % whereas when we took 1.5mg/ml and 2 mg/ml of the drug the EE was calculated as 3.1% and 3.7%. So, the maximum encapsulation was found in 1 mg/ml concentration.

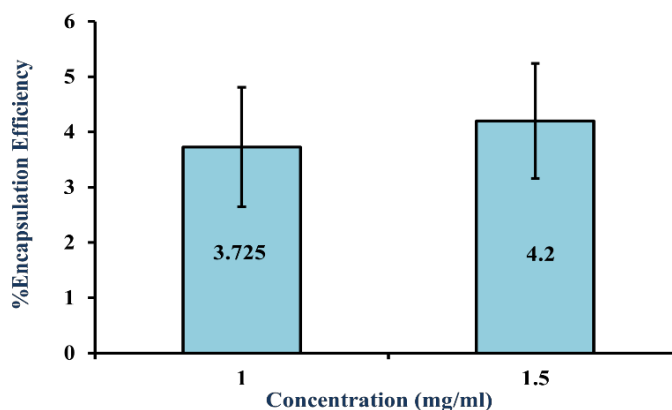


Figure 22: Drug encapsulation for Timolol Maleate in chitosan nanoparticles

4.6. *In vitro* drug release study of Pilocarpine from BSA and Chitosan nps

The drug release study was done to study the amount of drug released from the nanoparticles at a particular interval of time. In Pilocarpine-loaded BSA nanoparticles, nearly 85% of cumulative drug release was seen at 360 minutes whereas in Pilocarpine-loaded chitosan nanoparticles same amount of drug release at 300 minutes. This shows that more sustain of drug release was seen in PLC-loaded BSA nanoparticles as compared to PLC-loaded chitosan nanoparticles.

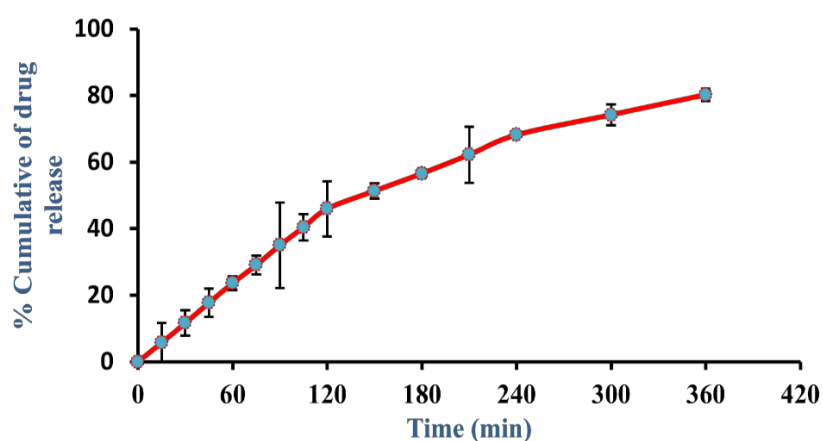


Figure 23 : *In- vitro* drug release of pilocarpine from BSA nanoparticle

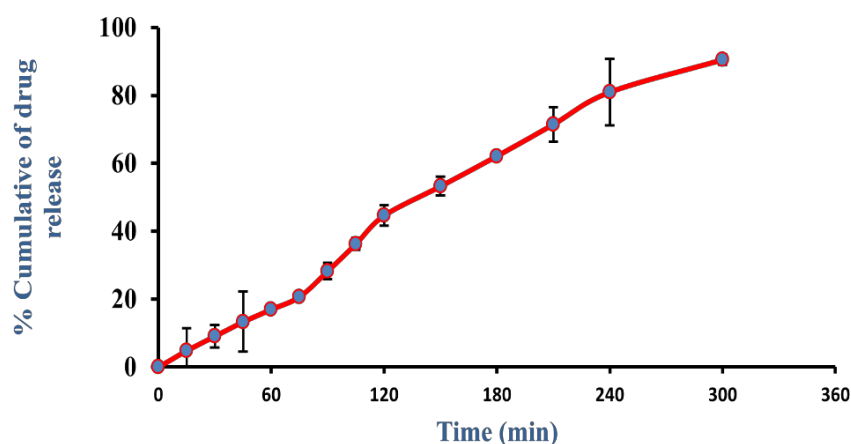


Figure 24 : *In- vitro* drug release of pilocarpine from chitosan Nps

4.7. Finding optimal concentration gellan gum

To determine the optimal concentration of gellan gum for our application, we aimed to achieve a solution with low viscosity for ease of dropwise flow while ensuring high viscosity upon gelation in the presence of tear fluid ions. We prepared gellan gum solutions at concentrations of 0.25%, 0.5%, and 0.75% (w/v) in ultrapure water and subsequently measured their viscosities across a range of shear rates to assess their flow properties. Our findings indicated that the 0.25% gellan gum solution exhibited the lowest viscosity, facilitating easy flow, while the 0.75% solution displayed significantly higher viscosity in solution form. To evaluate the gelation behavior, we introduced simulated tear fluid (STF) to each solution, allowing the ionic components to induce gel formation. Upon measuring the viscosity of the resulting gels, we observed that the viscosities of the 0.25% and 0.5% gellan gum gels were comparable, whereas the 0.75% gellan gum gel demonstrated the highest viscosity. Based on these results, we selected the 0.25% gellan gum concentration as the optimal formulation, as it provided the lowest viscosity in solution form—ensuring ease of administration—while achieving a high viscosity upon gelation, making it suitable for our intended application.

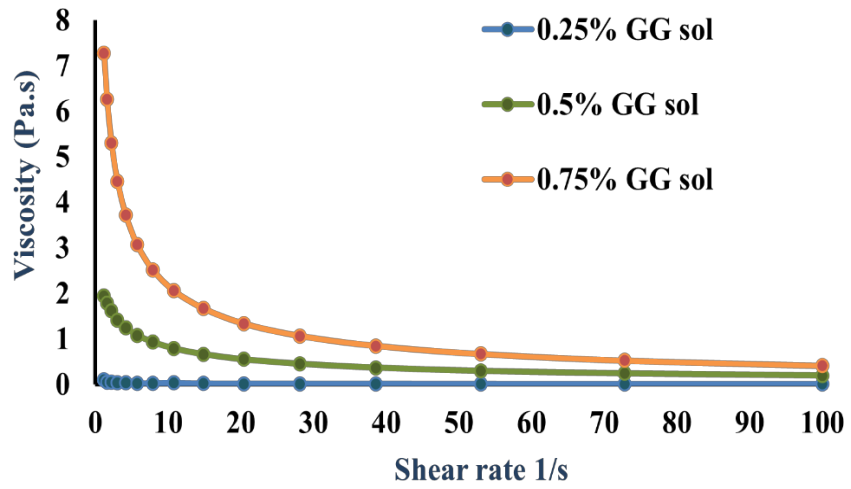


Figure 25: Viscosity as a function of shear rate of different concentration of GG solution

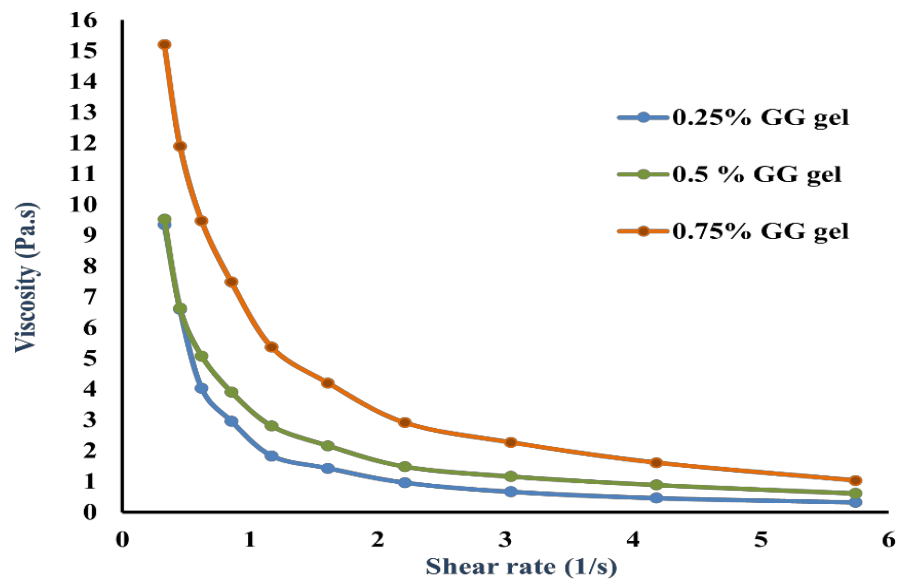


Figure 26: Viscosity as a function of shear rate of different concentration of GG solution after adding STF

4.8. Gelation studies

In this study, we aimed to investigate whether the gelation behavior of gellan gum is influenced by pH or ionic concentration. To explore this, 10 mL aliquots of various pH buffer solutions were prepared, including pH 4, pH 6, pH 7, pH 9, simulated tear fluid, and distilled water, each contained in separate glass bottles. To initiate the gelation process, 1 mL of a 0.25% gellan gum solution was added to each of the prepared buffer solutions. Since gellan gum is inherently transparent, methylene blue dye was incorporated into the solutions to visually monitor the gelation process. Upon observation, gel formation was noted in all the buffer solutions with varying pH levels (pH 4, pH 6, pH 7, pH 9, and simulated tear fluid). However, in distilled water, no gel formation occurred. This observation suggests that the gelation of gellan gum is not strongly pH-dependent, as gel formation occurred across all pH conditions tested. Instead, the results indicate that gelation may be more closely related to the presence of ions in the solution. The lack of gel formation in distilled water, which is devoid of ions, supports the hypothesis that ionic strength plays a crucial role in the gelation process of gellan gum. Therefore, it can be concluded that gellan gum gelation is ion-sensitive rather than pH-sensitive.

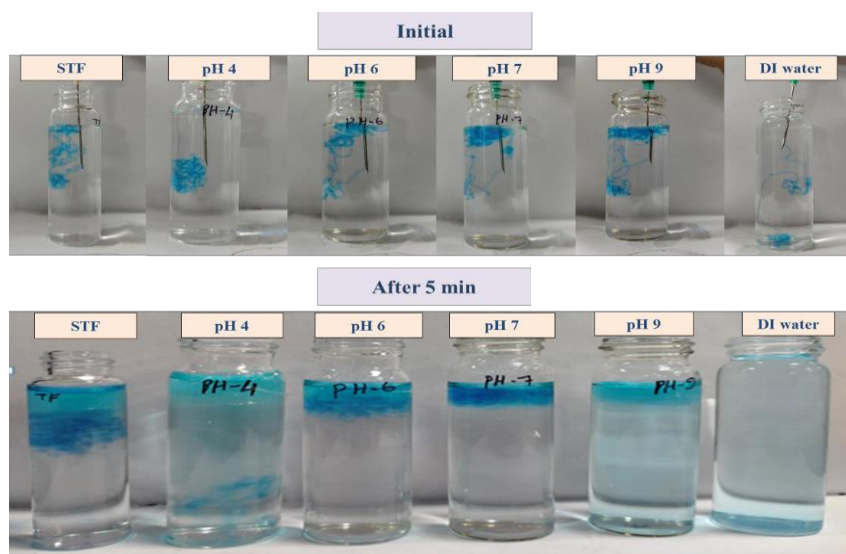


Figure 27 : Gelation studie of gellan gum in different pH

4.9. Interaction between different nanoparticle

In this study, we investigated the interaction between gellan gum solution and different nanoparticles, specifically bovine serum albumin (BSA) nanoparticles and chitosan nanoparticles, by assessing changes in viscosity. To evaluate these interactions, BSA and chitosan nanoparticles were incorporated into the gellan gum solution, and the viscosity of the resulting mixtures was measured. Our results indicated that the addition of nanoparticles did not cause any significant change in the viscosity of the gellan gum solution, suggesting that their presence did not alter the solution's rheological properties. To further assess the impact of nanoparticles on gelation behavior, we introduced simulated tear fluid (STF) into the nanoparticle-containing gellan gum solutions, allowing gel formation via ionic crosslinking. The viscosity of the resulting gels was then measured and compared to that of plain gellan gum gel. Our findings revealed that the viscosity remained unchanged across all formulations, indicating that the incorporation of BSA and chitosan nanoparticles did not influence the gel's rheological properties. These results suggest that the nanoparticles do not interfere with the gelation

process of gellan gum in the presence of tear fluid ions, maintaining similar viscosity profiles in both solution and gel states.

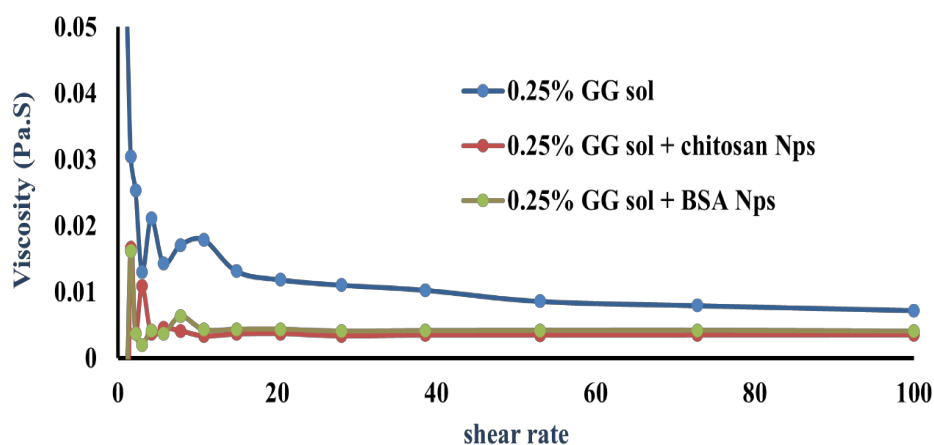


Figure 28: Viscosity as a function of shear rate of GG solution with different Nps

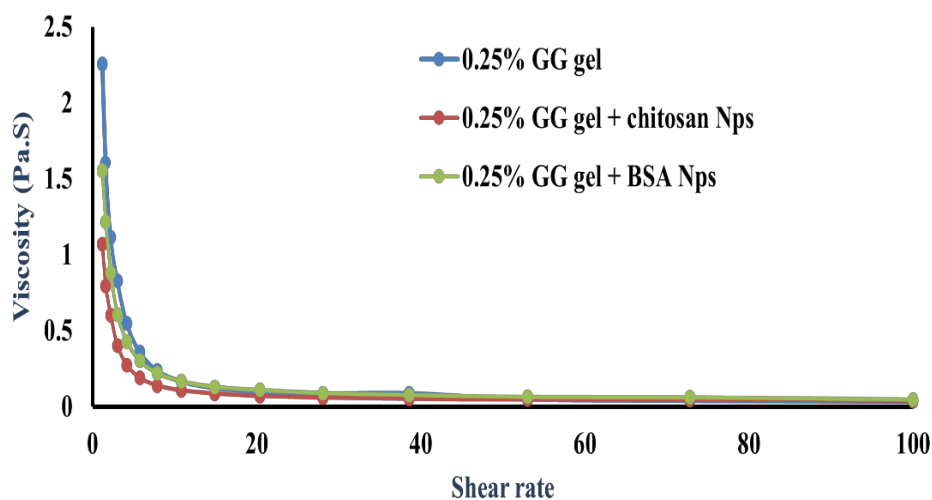


Figure 29: Viscosity as a function of shear rate of GG solution with different Nps after adding STF

4.10. Entrapment efficiency of pilocarpine and timolol maleate in gellan gumgel

The encapsulation efficiency of pilocarpine and timolol maleate was evaluated by incorporating the drug at a concentration of 1 mg/mL into the two different gellan gum solution. The percentage of drug entrapment was then determined to assess the efficiency of drug loading within the gellan gum matrix. Upon analysis, it was observed that when 1 mg/mL

of pilocarpine was used, the entrapment efficiency was found to be 70%. In other hand 1mg/ml of timolol maleate was used then the entrapment efficiency was 91%. This high entrapment efficiency indicates the effective incorporation of the drug within the gellan gum system, making it a promising formulation for controlled drug delivery.

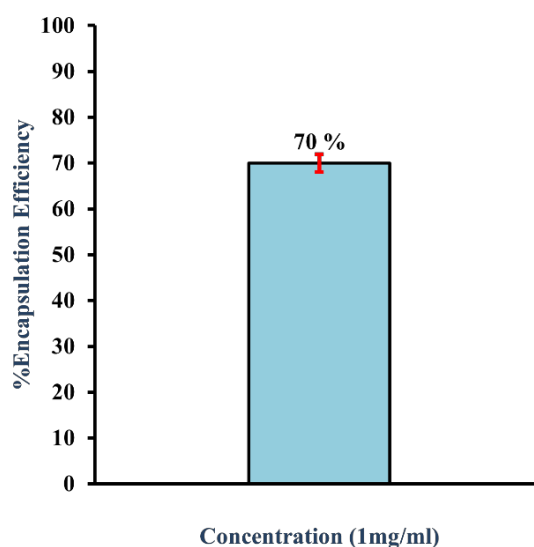


Figure 30 : Graphical representation of drug encapsulation for pilocarpine in Gellan gum gel

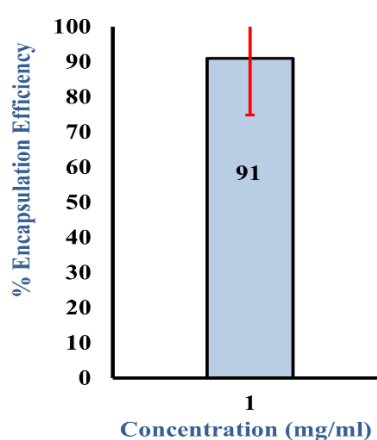


Figure 31 : Graphical representation of drug encapsulation for Timilol maleate in Gellan gum gel.

4.11. *In vitro* drug release of pilocarpine & Timolol maleate from gellan gum

The drug release study was done to study the amount of drug released from the gellan gum gel at a particular interval of time. In Pilocarpine loaded gel, nearly 95% of cumulative drug release was seen at 600 minutes whereas in timolol maleate loaded gellan gum gel, 80% of drug release at 150 minutes. This shows that more sustain of pilocarpine drug release was seen in PLC-loaded gellan gum gel as compared to timolol maleate loaded gellan gum gel.

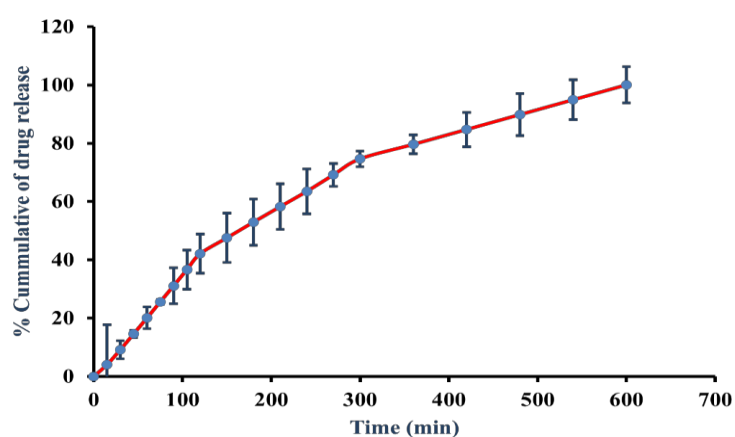


Figure 32 : Graphical representation of *In vitro* drug release of pilocarpine Gellan gum gel

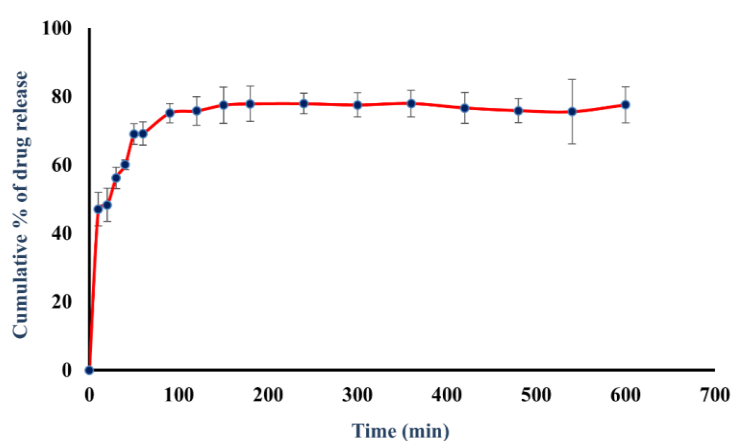


Figure 33 : Graphical representation of *In vitro* drug release of timolol maleate Gellan gum gel

4.12. Drug release profile of dual drug

To achieve sustained drug release, a combination therapy approach was employed by incorporating two different drugs within a single gellan gum gel formulation. Timolol Maleate was directly incorporated into the gellan gum gel, while Pilocarpine Hydrochloride was first encapsulated within bovine serum albumin (BSA) nanoparticles, which were then dispersed within the gellan gum gel. This dual-drug delivery system was designed to optimize the release profiles of both drugs, ensuring prolonged therapeutic effects. The *in vitro* drug release study demonstrated that Timolol Maleate exhibited an 80% release within 150 minutes, indicating a relatively faster release profile. In contrast, Pilocarpine Hydrochloride, which was encapsulated within BSA nanoparticles and subsequently incorporated into the gellan gum gel, exhibited a sustained release pattern, with 85% of the drug being released over 600 minutes. This prolonged release of Pilocarpine can be attributed to the nanoparticle-mediated encapsulation, which provided a controlled and gradual release from the gel matrix. These findings highlight the potential of the developed formulation for sustained ocular drug delivery, effectively extending the therapeutic window and reducing the frequency of administration.

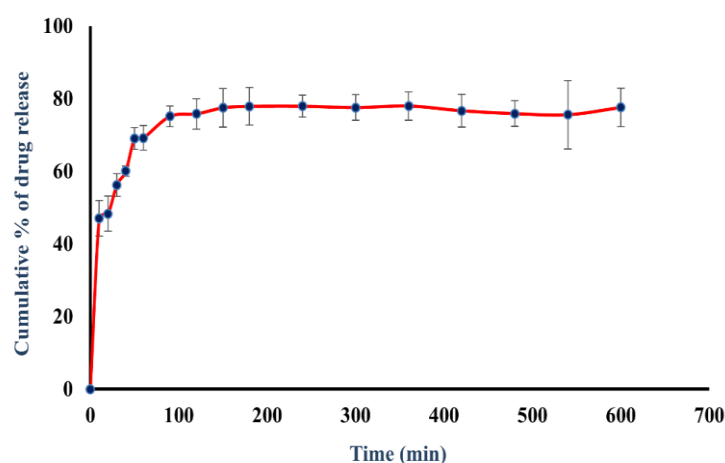


Figure 34 : Graphical representation of *In vitro* drug release of TM from gel

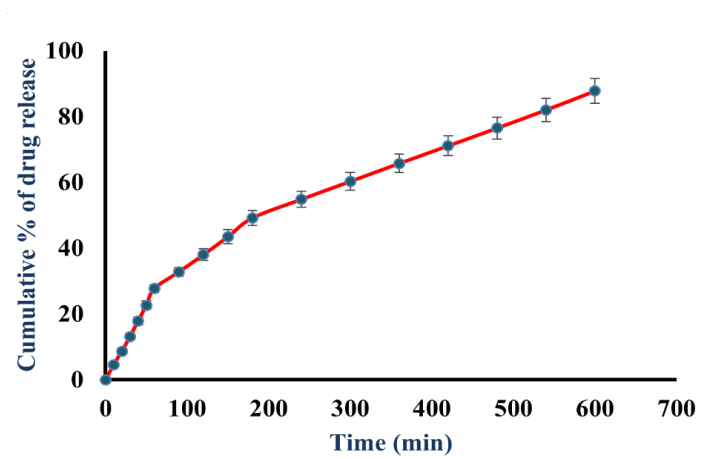


Figure 35 : Graphical representation of *In vitro* drug release of plc from Nps and gel

4.13. *In Vitro* cell toxicity by MTT analysis

The cytotoxic effects of the nanoparticle were evaluated using a colorimetric MTT assay, which measures cell viability. In this test, the yellow MTT compound (3-(4,5-dimethylthiazol-2-yl)-2,5-diphenyltetrazolium bromide) is metabolized by cellular NADPH-dependent oxidoreductase enzymes into insoluble purple formazan crystals. These crystals are then dissolved with DMSO, producing a colored solution whose intensity is measured by absorbance at 570 nm using a spectrophotometer. At lower concentrations, the nanoparticles showed minimal or no toxicity to HEK 293 healthy kidney cells. However, as the concentration of the nanoparticle increased, a gradual reduction in cell viability was observed.

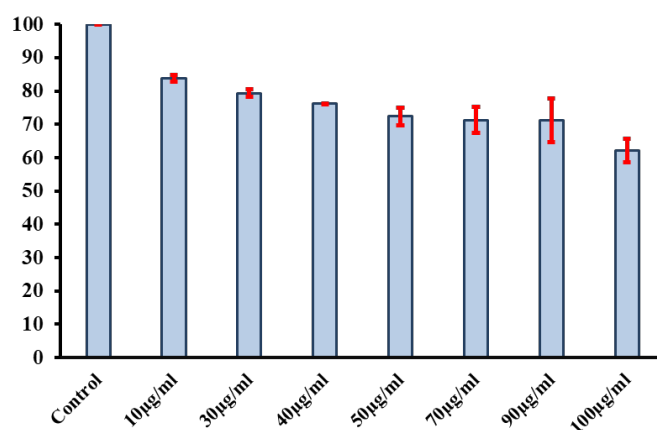


Figure 36 : The percentage of cell viability of drug loaded nanoparticle on HEK 293 cell

4.14. *Ex-vivo* transcorneal permeation study

Ex-vivo transcorneal permeation studies conducted on the newly developed formulation demonstrated a significantly greater drug permeation through the goat cornea upto 6 hours compared to both the plain drug solution. These findings underscore the potential advantages of gellan gum in ocular formulations to improve therapeutic efficacy. In the drug permeation study, pilocarpine solution alone demonstrated approximately 70% drug permeation within 1 hour, indicating rapid release and absorption. However, when pilocarpine was incorporated into a gellan gum-based formulation, the same extent of drug permeation (approximately 70%) was observed over a prolonged period of 6 hours. When timolol maleate was incorporated in gellan gum based formulation 85% percent of drug permeate in 5 hours. This significant delay in drug release suggests that the gellan gum matrix effectively sustained the release of pilocarpine, thereby highlighting its potential as a controlled-release ocular delivery system.

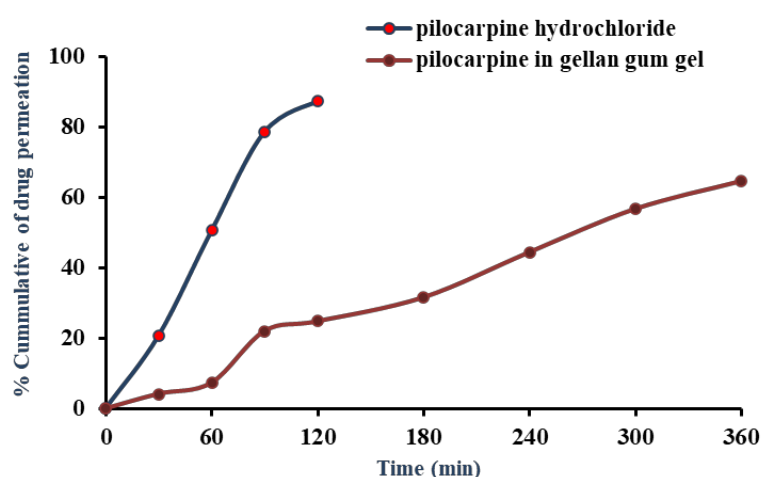


Figure 37 : Transcorneal permeation study of only pilocarpine hydrochloride and pilocarpine loaded in gellan gum using goat cornea

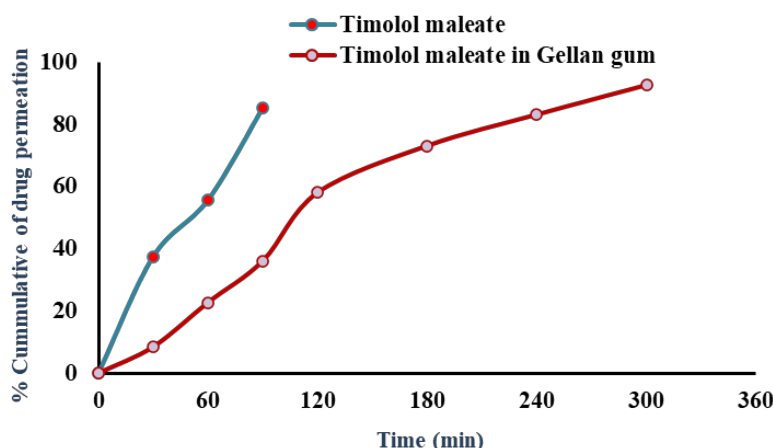


Figure 38 : Transcorneal permeation study of only pilocarpine hydrochloride and pilocarpine loaded in gellan gum using goat cornea

4.15. Mucoadhesive study using flow of tear fluid

The mucoadhesive properties of gellan gum gel were evaluated through flow of simulated tear fluid. In this study, gellan gum solution was applied on excised corneal tissues, followed by continuous perfusion with simulated tear fluid (STF). The gel remained adhered to the corneal surfaces for up to 2 hours, indicating strong resistance to wash-off under simulated physiological conditions.

4.16. Evaluate the adhesive force between cornea and in-situ gel

In this study, the mechanical strength of the cornea–gel interface was assessed using a weight-based detachment test. Initially, two corneal tissues were placed in contact without any gel between them, and weights were incrementally applied to one side of the setup. Detachment occurred at a load of approximately 250–260 mg, indicating weak natural adhesion. In contrast, when gellan gum gel was placed between the corneal tissues, the system was able to withstand significantly higher

loads, ranging from 1800 to 2000 mg, before detachment. This increase in tolerance is attributed to the mucoadhesive properties of gellan gum, which enhanced the interaction between the gel and the corneal surface. Notably, the maximum tolerated load in the presence of the gel exceeded the average human blink force (~1600 mg), suggesting the formulation's potential to resist mechanical stresses during blinking.

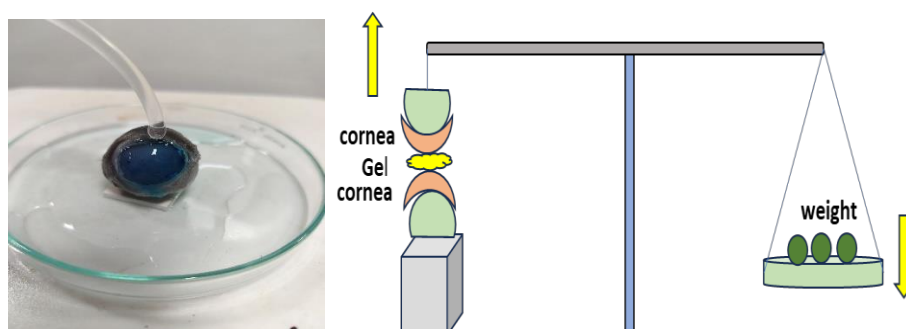


Figure 39 : Graphical representation of mucoadhesive test

Chapter 5

5. Conclusions

Glaucoma is an eye condition characterized by increased intra-ocular pressure which leads to irreversible damage of optic nerves. If not treated glaucoma can result in permanent eye vision loss. Current treatments for glaucoma involve eye drop medications, that have significant limitations such as the need for frequent doses and reduced precorneal retention time. This report discusses the various conventional glaucoma medications and explores how their effectiveness can be enhanced using different nanoparticles like bovine serum albumin nanoparticles and chitosan nanoparticles and gellan gum gel. Over time, numerous strategies have been developed to achieve sustained or controlled drug release to the eye. These advanced delivery methods hold promise for improving patient adherence, enhancing drug efficacy, minimizing side effects, and ultimately preserving the vision of individuals with glaucoma. In conclusion of our works, we synthesized insitu gel having drug loaded nanoparticles, which shows higher drug encapsulation with sustain drug release, and also greater drug permeation because of mucoadhesive in-situ gel , which helps more bioavailability of drug, less dose concentration, less dose frequency compare to the conventional eye drops.

REFERENCES

- [1] R. Sihota, D. Angmo, D. Ramaswamy, and T. Dada, "Simplifying "target" intraocular pressure for different stages of primary open-angle glaucoma and primary angle-closure glaucoma," *Indian journal of ophthalmology*, vol. 66, no. 4, pp. 495-505, 2018.
- [2] N. J. Wade, *A natural history of vision*. MIT press, 2000.
- [3] A. R. Stothert, S. N. Fontaine, J. J. Sabbagh, and C. A. Dickey, "Targeting the ER-autophagy system in the trabecular meshwork to treat glaucoma," *Experimental eye research*, vol. 144, pp. 38-45, 2016.
- [4] C. Henein, "Glaucoma drainage devices: design, flow resistance and biocompatibility implications for intraocular pressure control," UCL (University College London), 2021.
- [5] H. A. Quigley, R. W. Flower, E. M. Addicks, and D. S. McLeod, "The mechanism of optic nerve damage in experimental acute intraocular pressure elevation," *Investigative ophthalmology & visual science*, vol. 19, no. 5, pp. 505-517, 1980.
- [6] M. N. Cyrlin, T. Filippopoulos, and C. L. Grosskreutz, "Primary and secondary angle-closure glaucomas," in *Clinical Glaucoma Care: The Essentials*: Springer, 2013, pp. 287-322.
- [7] N. A. Loewen and A. P. Tanna, "Glaucoma risk factors: Intraocular pressure," in *Clinical Glaucoma Care: The Essentials*: Springer, 2013, pp. 1-22.
- [8] I. Goldberg, "Drugs for glaucoma," *Australian Prescriber*, vol. 25, no. 6, 2002.
- [9] S. R. Salunke and S. B. Patil, "Ion activated in situ gel of gellan gum containing salbutamol sulphate for nasal administration," *International journal of biological macromolecules*, vol. 87, pp. 41-47, 2016.
- [10] R. C. Tseng, C.-C. Chen, S.-M. Hsu, and H.-S. Chuang, "Contact-lens biosensors," *Sensors*, vol. 18, no. 8, p. 2651, 2018.

- [11] C. Fiorica, G. Biscari, F. S. Palumbo, G. Pitarresi, A. Martorana, and G. Giammona, "Physicochemical and rheological characterization of different low molecular weight gellan gum products and derived ionotropic crosslinked hydrogels," *Gels*, vol. 7, no. 2, p. 62, 2021.
- [12] V. D. Prajapati, G. K. Jani, B. S. Zala, and T. A. Khutliwala, "An insight into the emerging exopolysaccharide gellan gum as a novel polymer," *Carbohydrate polymers*, vol. 93, no. 2, pp. 670-678, 2013.
- [13] I. D. Rupenthal, C. R. Green, and R. G. Alany, "Comparison of ion-activated in situ gelling systems for ocular drug delivery. Part 1: physicochemical characterisation and in vitro release," *International journal of pharmaceutics*, vol. 411, no. 1-2, pp. 69-77, 2011.
- [14] Y. Yao *et al.*, "Nanoparticle-based drug delivery in cancer therapy and its role in overcoming drug resistance," *Frontiers in molecular biosciences*, vol. 7, p. 193, 2020.
- [15] A. M. Qandil, T. J. Marjic, B. M. Al-Taani, A. H. Khalede, and A. A. Badwan, "Depolymerization of HMW into a predicted LMW chitosan and determination of the degree of deacetylation to guarantee its quality for research use," *Journal of Excipients & Food Chemicals*, vol. 9, no. 2, 2018.
- [16] S. Phunpee *et al.*, "Controllable encapsulation of α -mangostin with quaternized β -cyclodextrin grafted chitosan using high shear mixing," *International Journal of Pharmaceutics*, vol. 538, no. 1-2, pp. 21-29, 2018.
- [17] R. M. Hathout *et al.*, "Gelatinized core liposomes: A new Trojan horse for the development of a novel timolol maleate glaucoma medication," *International Journal of Pharmaceutics*, vol. 556, pp. 192-199, 2019.
- [18] S. Yu *et al.*, "Liposome incorporated ion sensitive in situ gels for ocular delivery of timolol maleate," *International journal of pharmaceutics*, vol. 480, no. 1-2, pp. 128-136, 2015.

- [19] R. Zhao, J. Li, J. Wang, Z. Yin, Y. Zhu, and W. Liu, "Development of timolol-loaded galactosylated chitosan nanoparticles and evaluation of their potential for ocular drug delivery," *AAPS PharmSciTech*, vol. 18, pp. 997-1008, 2017.
- [20] R. Ilka, M. Mohseni, M. Kianirad, M. Naseripour, K. Ashtari, and B. Mehravi, "Nanogel-based natural polymers as smart carriers for the controlled delivery of Timolol Maleate through the cornea for glaucoma," *International journal of biological macromolecules*, vol. 109, pp. 955-962, 2018.
- [21] H. A. Salama, M. Ghorab, A. A. Mahmoud, and M. Abdel Hady, "PLGA nanoparticles as subconjunctival injection for management of glaucoma," *Aaps Pharmscitech*, vol. 18, pp. 2517-2528, 2017.
- [22] V. Dubey, P. Mohan, J. S. Dangi, and K. Kesavan, "Brinzolamide loaded chitosan-pectin mucoadhesive nanocapsules for management of glaucoma: Formulation, characterization and pharmacodynamic study," *International journal of biological macromolecules*, vol. 152, pp. 1224-1232, 2020.
- [23] B. Joshi, J. Kaur, E. Khan, A. Kumar, and A. Joshi, "Ultrasonic atomizer driven development of doxorubicin-chitosan nanoparticles as anticancer therapeutics: Evaluation of anionic cross-linkers," *Journal of Drug delivery science and technology*, vol. 57, p. 101618, 2020.